WSRC-TR-2002-00333
Revision 0

THE INFLUENCE OF SOIL-STRUCTURE-INTERACTION ON THE INELASTIC FORCE REDUCTION FACTOR, Fμ (U)

July 2002

Structural Mechanics
Westinghouse Savannah River Company
Savannah River Site
Aiken, SC 29808

WSRC-TR-2002-00333
Revision 0

THE INFLUENCE OF SOIL-STRUCTURE-INTERACTION ON THE INELASTIC FORCE REDUCTION FACTOR, Fμ (U)

By

Greg E. Mertz
Westinghouse Savannah River Company

Review and Approved by: Fred Loceff 8.5.2002
Fred Loceff

Summary

An inelastic force reduction factor, Fμ, has been proposed for use in a performance based standard for the seismic design of nuclear facilities. Throughout the development of Fμ is the implicit assumption that ductility is distributed throughout the structure's load path. The adverse consequences of concentrating all of the structure's ductility in a single story have been noted by many researchers. It was unknown whether Soil-Structure-Interaction (SSI) effects could cause similar adverse consequences in shear wall structures common to nuclear facilities.

A limited study is performed in this paper to determine the effects of soil-structure-interaction on the inelastic response of reinforced concrete shear wall structures. The inelastic force reduction factor, Fμ, is calculated for shear walls with and without the effects of soil flexibility by comparing the calculated elastic to nonlinear responses. Consistent with FEMA-273 and the draft standard, wall damage is expressed by a single parameter, shear strain. Nonlinear deformations are limited to the shear walls.

For the structures examined, Soil Structure Interaction did not significantly affect the magnitude of wall shear strain. Thus, Soil-Structure-Interaction (SSI) effects do not cause adverse consequences in shear wall structures common to nuclear facilities.

SSI did cause a reduction in Fμ. This reduction is not due to a concentration of damage in the shear wall. Rather, this reduction is due to the reduction in elastic response as soil damping is introduced. Overall, the Fμ proposed by the draft standard are generally conservative for both fixed base and SSI structures.

Table of Contents

Summary iii
1.0 Introduction 1
2.0 Analytical Approach 2
2.1 Ground Motion 2
2.2 Super Structure Model 2
2.3 Soil Structure Interaction Model 4
2.4 Fμ 5
2.5 Analysis Methodology 5
3.0 Discussion of Results 15
3.1 Fμ For Various Shear Strains 15
3.2 Influence of SSI on Wall Damage 16
3.3 Cause of Fμ Reduction for SSI Systems 17
3.4 Estimated versus Calculated Fμ 17
3.5 Influence of Elastic Structure Damping on Fμ 18
3.6 Influence of Nonlinear Structure Damping on Fμ 19
3.7 Frequency Content of Structures with Nonlinear Behavior 20
3.8 Correlation Between Input Energy and Shear Strain 21
4.0 Summary and Conclusion 45
5.0 References 46

1.0 Introduction

An inelastic force reduction factor, Fμ, has been proposed for use in a performance based standard for the seismic design of nuclear facilities [1] which is an extension of the inelastic force reduction factor currently used to design DOE structures [2]. Throughout the development of Fμ is the implicit assumption that ductility is distributed throughout the structure's load path. The adverse consequences of concentrating all of the structures ductility in a single story have been noted by many researchers and an approach to reduce Fμ for a soft or weak story is included in the draft standard [1].

Fμ are typically developed for a structure resting on rock, or for free-field soil motions where the free-field motion includes amplification due to the soil column [7]. None of the Fμ currently in the draft standard explicitly include interaction effects between the soil and structure. One proposed approach to incorporating SSI effects is to assume that the inelastic energy dissipation will be concentrated in the structure and the structure's ductility demand is similar to the ductility demand in a weak story. Utilizing the weak story approach for a one story structure on soil springs reduces the inelastic force reduction factor to $^{(2+F\mu)}/_{3}$, which is quite a severe penalty.

Implicit in the weak story Fμ reduction is the assumption that concentrating all of the inelastic action in one part of the load path increases the damage in that part of the load path. The following limited study shows that SSI does not significantly increase the damage in a reinforced concrete shear wall structure. Thus, the behavior which the weak story Fμ reduction was developed to represent is not present in the shear wall – SSI problem.

A limited study is performed in this paper to determine the effects of soil-structure-interaction on the inelastic force reduction factor, Fμ, for reinforced concrete shear wall structures.

2.0 Analytical Approach

The effects of SSI on the inelastic force reduction factor, Fμ, for reinforced concrete shear wall structures are evaluated by comparing the dynamic response of shear walls with and with-out SSI. The shear wall stiffness used in this study is based on experimental results. Shear walls with natural frequencies of 5 and 8 hz are considered. Soil Structure Interaction is represented by lumped parameter soil springs, which are tuned to yield SSI frequencies of approximately 3 and 5 hz. The study uses a single broad energy ground motion as input.

2.1 Ground Motion

The input ground motion is based on a 5% damped, median NUREG/CR-0098 spectra [3] with a target peak ground acceleration of 1g. Acceleration, velocity and displacement time histories are shown in Figures 2.1 through 2.3. Peak accelerations, velocities and displacements are summarized in Table 2.1. The acceleration response spectra is compared to the 5% damped NUREG CR-0098 target in Figure 2.4. Acceleration response spectra for various damping are shown in Figure 2.5.

Note that the input motion is a broad design motion and is not typical of real earthquake time histories. The response spectra for real earthquake time histories have numerous peaks and valleys. The nonlinear response from a real time history is believed to be less than the response from the broad design motion used in this study.

Table 2.1 Peak Ground Motion Parameters

	Peak Value	**Target Value**
Acceleration	1.0063g	1 g
Velocity	43.87 in/sec	48 in/sec
Displacement	28.31 in	35.7748 in

2.2 Super Structure Model

Lateral loads, in this study, are resisted by an 18" thick, 40' wide by 20' tall shear wall which has a calculated lateral stiffness, K', of

$$K' = \frac{Ag\,G}{H} = 54{,}072 \text{ kip/inch}$$

where Ag is the total wall cross sectional area, Ag=480 in x 18 in = 8640 in^2,
H is the wall height, H=240 in,

G is the shear modulus for f'c=4000 psi concrete, $G = \frac{57\sqrt{f'c}}{2(1+\nu)} = 1502 \text{ ksi}$, and

ν is Poission's ratio, ν=0.2.

This wall is reinforced to have a nominal code capacity of $\phi Vn = \phi 6\sqrt{f'c}Ag = 3278$ kip with $\phi=1.0$.

The actual stiffness is based on the shear deformation of NCKU (National Cheng Kung University) wall SW6 [4, 5]. This isolated shear wall (no boundary elements) is 3.94 inch thick, 39.37 inch wide and 19.68 inch high (10 mm x 100 mm x 50 mm). Reinforcement is distributed evenly over the wall and consist of D13 (#4) bars with reinforcement ratios of $\rho h=1.03$ and $\rho v=0.77$. The steel yield strength is 69,535 psi with a concrete ultimate strength of 4087 psi. Wall SW6 was subject to cyclic static loading with an ultimate lateral load of 62 kips (28.11 metric tons) with a total deformation of 0.2695 inches (6.845 mm) of which 0.1529 inches (3.883 mm) is shear deformation. The shear backbone curve for wall SW-6 is shown in Figure 2.6. The load is converted into a normalized shear stress by dividing the load by $\sqrt{f'c}Ag$. Shear strain is the wall displacement divided by the height. The normalized shear stiffness backbone curve is shown in Figure 2.7 which has an ultimate drift ratio of 3.883/50=0.07766 at a shear stress of $6.23\sqrt{f'c}$.

The initial stiffness of Figure 2.7 changes at a shear stress of $1.33\sqrt{f'c}$ with a shear strain of 6.1864×10^{-5} (in/in). Thus, the initial stiffness, K, for the 40'x20' shear wall examined in this study, becomes

$$Pc = 1.33\sqrt{4000}Ag = 726.8 \text{ kip}$$
$$Dc = 6.1864 \times 10^{-5} H = 0.014847 \text{ in}$$

where Pc and Dc are the cracking load and displacement, respectively, and

$$K = \frac{Pc}{Dc} = 48{,}952 \ \frac{\text{kip}}{\text{in}}$$

which is within 10% of K' calculated above.

The fixed base structure, shown in Figure 2.8, is idealized as a single degree of freedom system with natural frequencies, fn, of 5 and 8 hz. The structural mass, M, is chosen to obtain these frequencies by

$$M = \frac{K}{(2\pi fn)^2}$$

A constant viscous damping, C, is assumed for both the elastic and nonlinear analyses. This damping is taken as 4% of the critical damping and is determined by

$$C = \rho 2\sqrt{K M}$$

where ρ is the damping ratio.

The nominal wall capacity is taken as $Vn = 6\sqrt{f'c}\,Ag = 3278\,\text{kip}$. Structural properties are summarized in Table 2.2.

Table 2.2 Structural Properties

	5 hz Structure	8 hz Structure
Elastic Stiffness, K	48,952 kip/in	48,952 kip/in
Viscous Damping, C	124.655 kip sec/in	77.909 kip sec/in
Mass, M	49.5987 kip sec^2/in	19.3745 kip sec^2/in
Weight, Wt	19,165 kip	7,486 kip
Nominal Capacity, Vn	3278 kip	3278 kip
Vn/Wt	0.171	0.438

A shear hysteresis model [4, 5] is used in this study to represent the nonlinear dynamic behavior of the reinforced concrete shear wall. This hysteresis model was developed as the mean fit to experimentally determined shear deformations from a series of isolated shear wall test. The shear hysteresis model has a curvilinear backbone curve and pinched hysteresis loops as shown in Figure 2.9. The model is compared to the cyclic response of shear wall SW-6 in Figure 2.10.

Bending deformation is neglected in this study. Bending deformation typically has hysteresis loops without the pinched behavior seen in Figures 2.9 and 2.10. Thus, bending deformation dissipates more energy than shear deformation and results in larger Fμ than shear deformation.

2.3 Soil Structure Interaction Model

The dynamic flexibility of the supporting soil is represented by a lumped parameter soil model consisting of a soil spring and dashpot, as shown in Figure 2.11. In an actual structure, the magnitude of soil stiffness is a function of building size, layer thickness, and high-strain dynamic soil properties.

In this study, the soil spring, Ks, is tuned such that the SSI frequency is about 5/8 of the fixed base structure frequency. The magnitude of SSI frequency is chosen to illustrate the general affects of SSI rather than to represent the actual SSI effects in a specific structure.

The foundation mass is assumed to be equal to the structural mass. Rigid Body SSI Damping ratios of 20%, 40% and 60% critical are considered. Again, the damping ratios are chosen to represent a range of SSI behaviors rather than the behavior of a specific structure. Viscous damping for the soil is determined by

$$Cs = \rho\, 2\sqrt{Ks\,(2\,M)}$$

The lumped parameter soil spring properties are summarized in Table 2.3.

Table 2.3 Lumped Parameter SSI Properties

	5 hz Structural Model	8 hz Structural Model
Soil Stiffness, Ks	50,754 kip/in	51,461 kip/in
SSI Frequency	3.131 hz	5.033 hz
20% Soil Viscous Damping, Cs	897.52 kip sec/in	564.84 kip sec/in
40% Soil Viscous Damping, Cs	1795.0 kip sec/in	1129.7 kip sec/in
60% Soil Viscous Damping, Cs	2692.6 kip sec/in	1694.5 kip sec/in

Elastic sine sweeps for the structures are shown in Figures 2.12 and 2.13. Both the shift in natural frequency due to soil flexibility and the reduction in peak amplification with increasing soil damping are evident in these figures.

2.4 Fμ

The inelastic force reduction factor, Fμ, is presented in the draft standard [1] as a component force modification factor that is used to reduce the elastically calculated member forces to account for nonlinear behavior. Thus, in application of the draft standard to a particular member, the elastically determined member force due to seismic loads, Ve, is reduced to represent the inelastic seismic force, Vn, by dividing Ve by Fμ;

$$Vn = \frac{Ve}{F\mu}$$

A common method of determining Fμ, consistent with the draft standard, is to take the ratio of the elastic to nonlinear force in a given member,

$$F\mu = \frac{Ve}{Vn} = \frac{\text{Elastic Member Force}}{\text{Nonlinear Member Force}}$$

This approach is utilized in this study.

Building codes for conventional structures reduce the elastically determined base shear for a structure by the response modification factor R. The base shear is then distributed over the height of the structure and the seismic forces are determined in individual elements. The response modification factor R includes both over-strength, Ro, and an inelastic force reduction factor for the structural system, Rμ. For the one degree of freedom structure evaluated in this study with a wall force equal to the base shear, Fμ=Rμ. Note that the draft standard has conservatively chosen to omit over-strength from it's response modification factors.

2.5 Analysis Methodology

The nonlinear dynamic response is calculated using the linear acceleration method with a time step of 0.0005 seconds using the approach in Reference 6. The program in

Reference 6 uses the same Raleigh damping coefficients for all elements and is modified to utilize dashpots to allow different damping values for the soil and structure.

An elastic analysis and multiple nonlinear analyses are performed for each structural model listed in Table 2.4. The elastic analysis is performed using the ≈1g PGA input acceleration. The ≈1g PGA input acceleration for each nonlinear run is scaled by a different factor, f to achieve various levels of seismic input. Thus, for each nonlinear analysis, the inelastic force reduction factor, Fμ, is calculated by

$$F\mu = \frac{\text{Elastic Wall Shear}}{\text{Nonlinear Wall Shear}} = \frac{f \times V_{Elastic1g}}{V_{Nonlinear\ (f)g's}}$$

where $V_{Elastic\ 1g}$ is the maximum elastic wall shear for 1g seismic input, and
$V_{Nonlinear\ (f)g}$ is the maximum nonlinear wall shear for f×1g seismic input.

Table 2.4 Structural Models

	Model	M $\frac{kip\ sec^2}{in}$	K $\frac{kip}{in}$	C $\frac{kip\,sec}{in}$	Ks $\frac{kip}{in}$	Cs $\frac{kip\,sec}{in}$	Fn hz
5 hz Structure	5 hz Fixed Base	49.5987	48,952	124.65	∞	0	5.0
	3.1 hz SSI w/ 20% Damping	49.5987	48,952	124.65	50,754	897.52	3.131
	3.1 hz SSI w/ 40% Damping	49.5987	48,952	124.65	50,754	1795.0	3.131
	3.1 hz SSI w/ 60% Damping	49.5987	48,952	124.65	50,754	2692.6	3.131
8 hz Structure	8 hz Fixed Base	19.3745	48,952	77.909	∞	0	8.0
	5 hz SSI w/ 20% Damping	19.3745	48,952	77.909	51,461	564.84	5.033
	5 hz SSI w/ 40% Damping	19.3745	48,952	77.909	51,461	1129.7	5.033
	5 hz SSI w/ 60% Damping	19.3745	48,952	77.909	51,461	1694.5	5.033

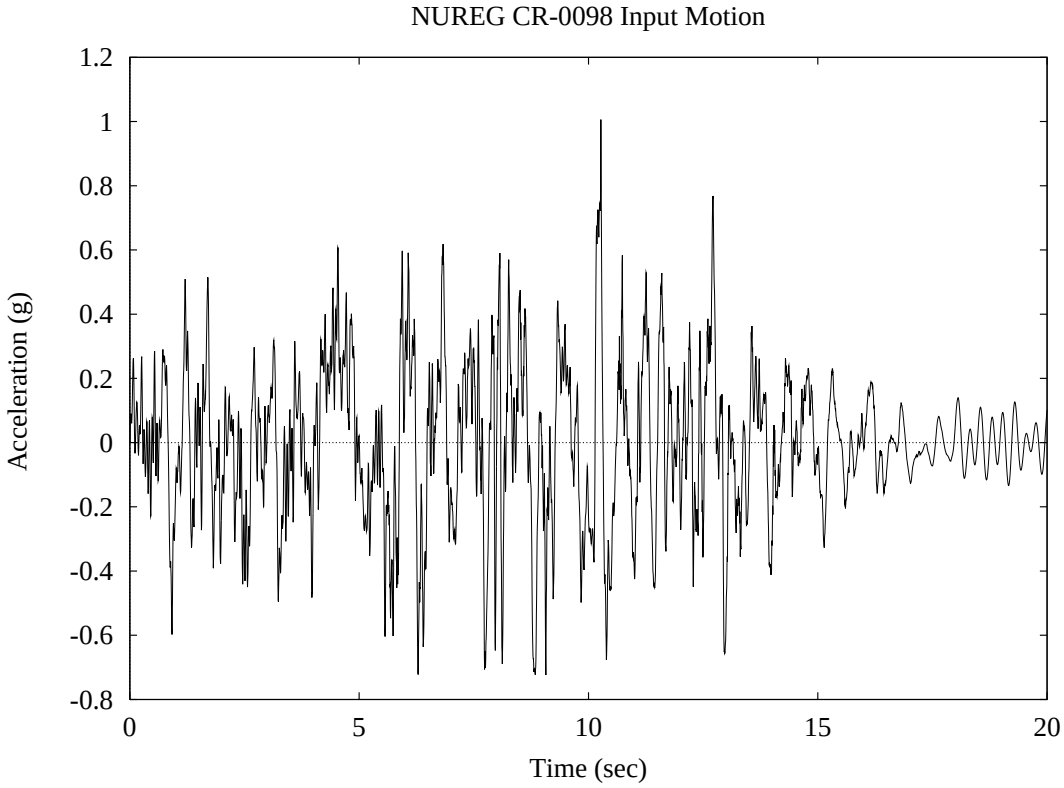

Figure 2.1 Input Acceleration Time History

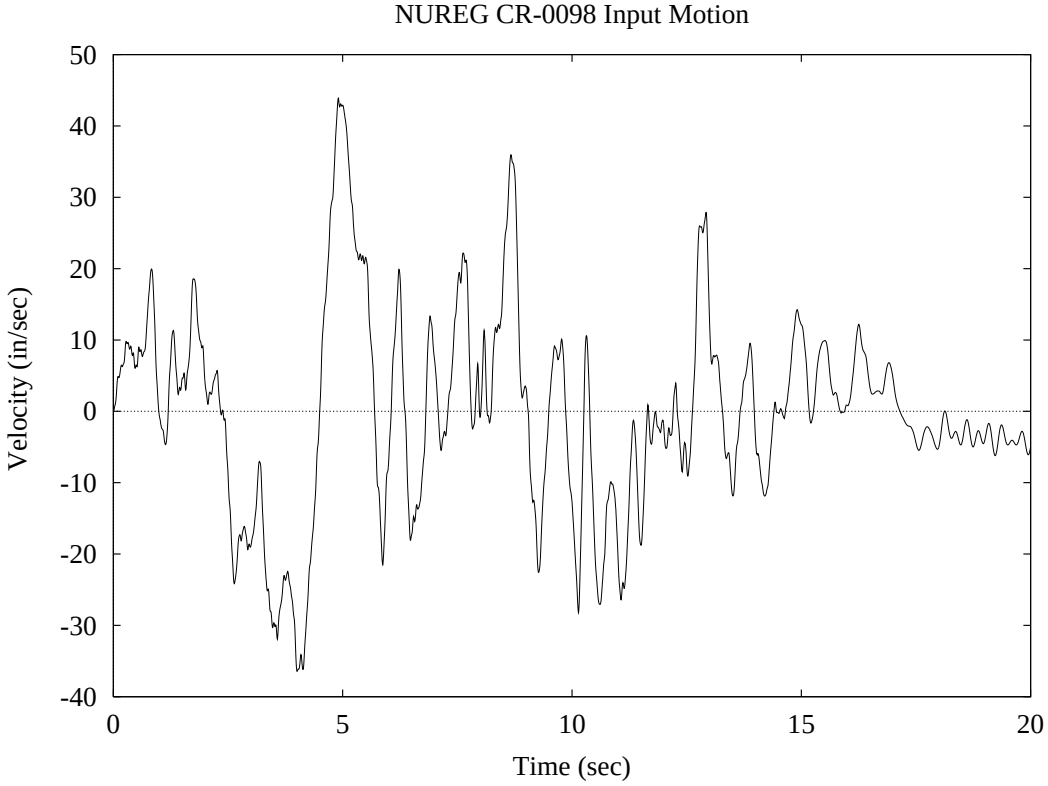

Figure 2.2 Input Velocity Time History

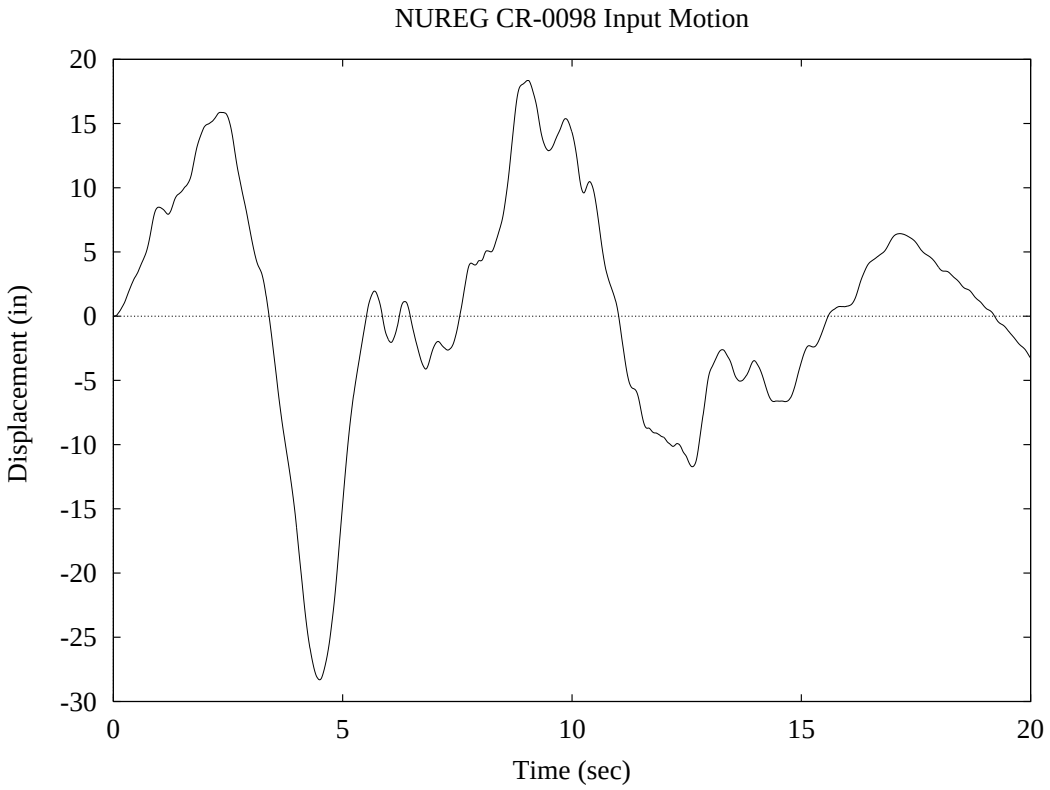

Figure 2.3 Input Displacement Time History

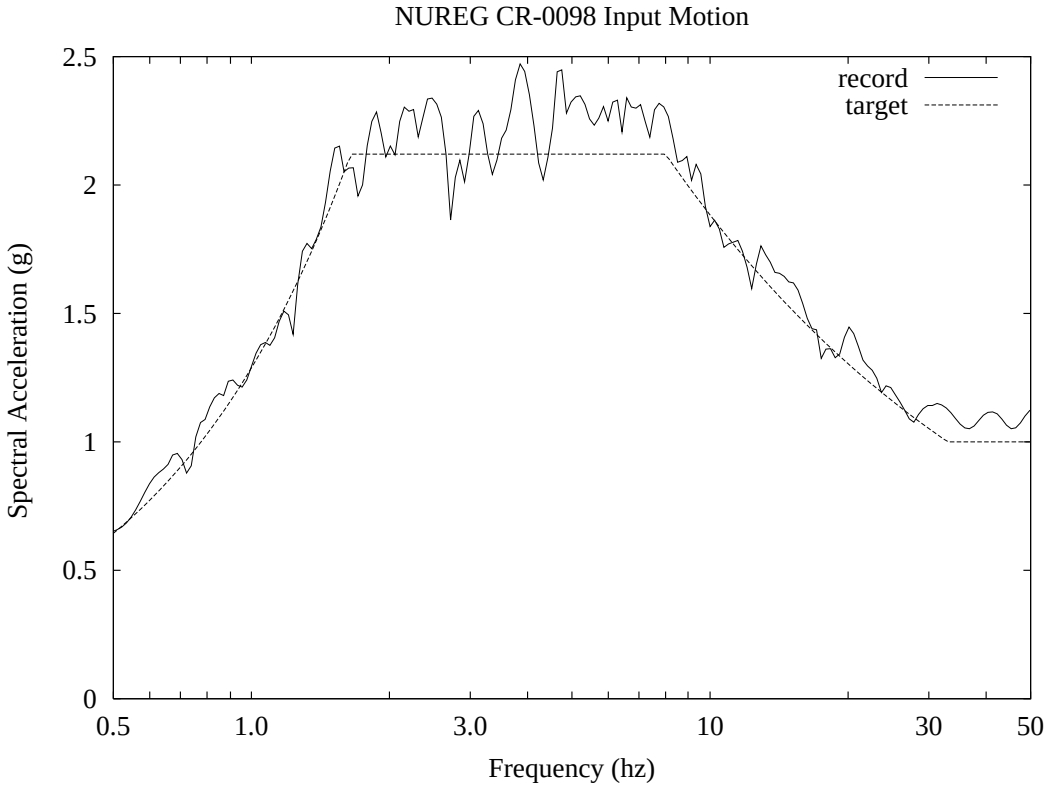

Figure 2.4 Input Acceleration 5% Response Spectra

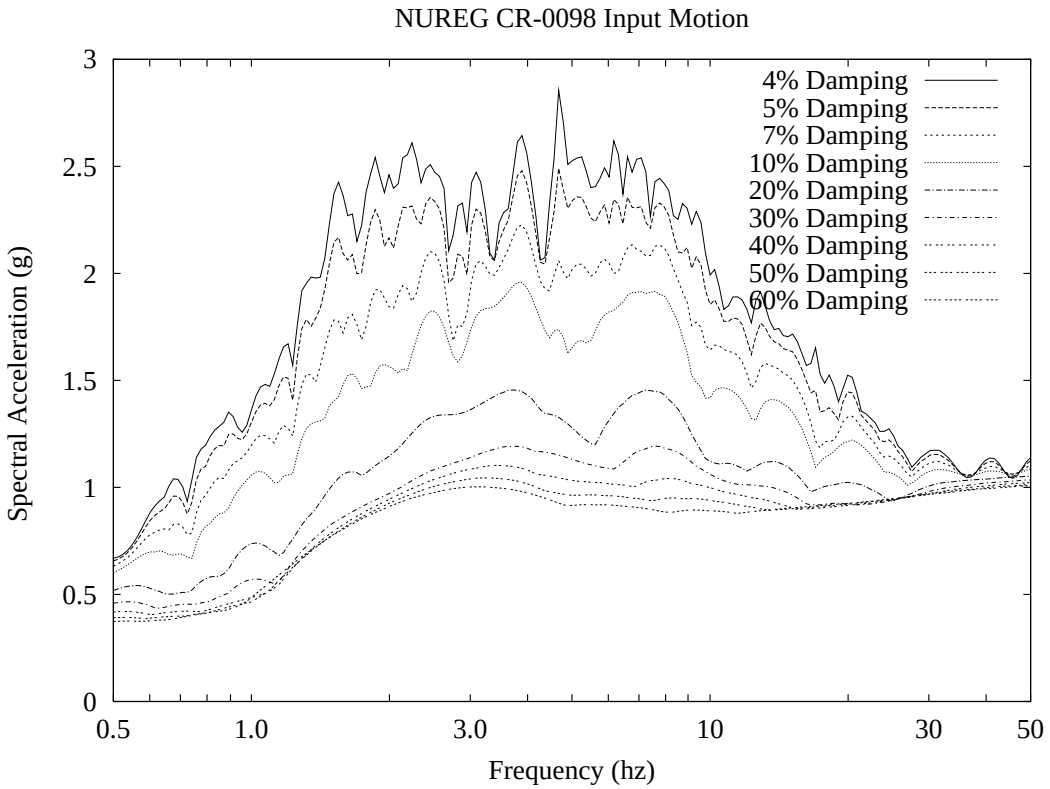

Figure 2.5 Input Acceleration Response Spectra

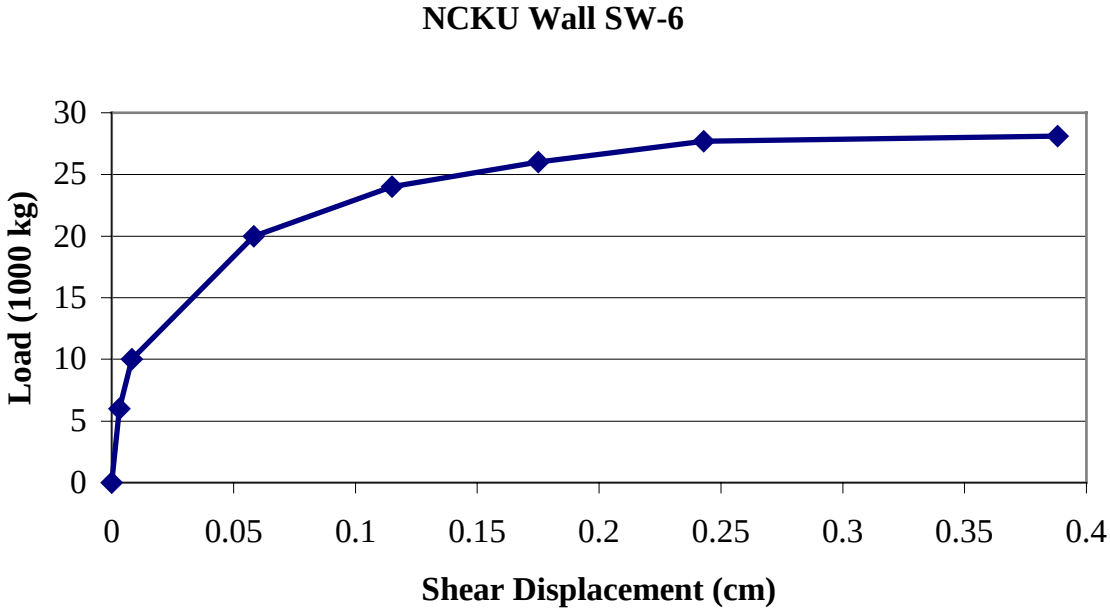

Figure 2.6 NCKU SW-6 Shear Backbone

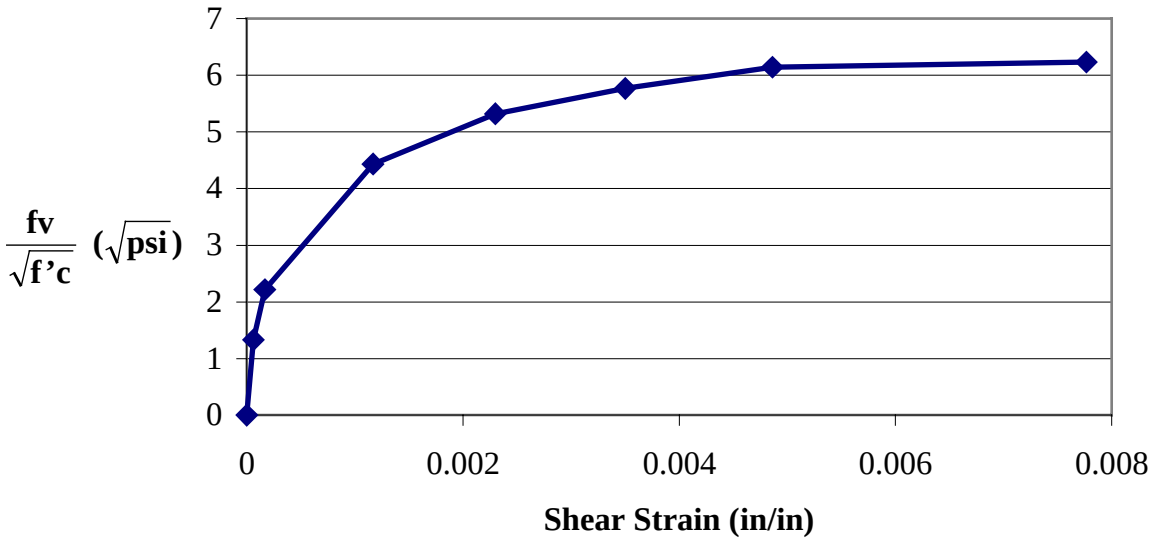

Figure 2.7 Normalized Shear Stiffness Backbone Curve

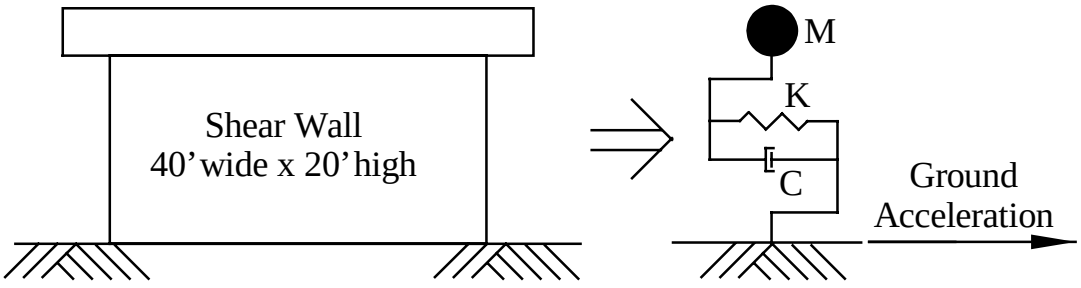

Figure 2.8 Fixed Base Structure

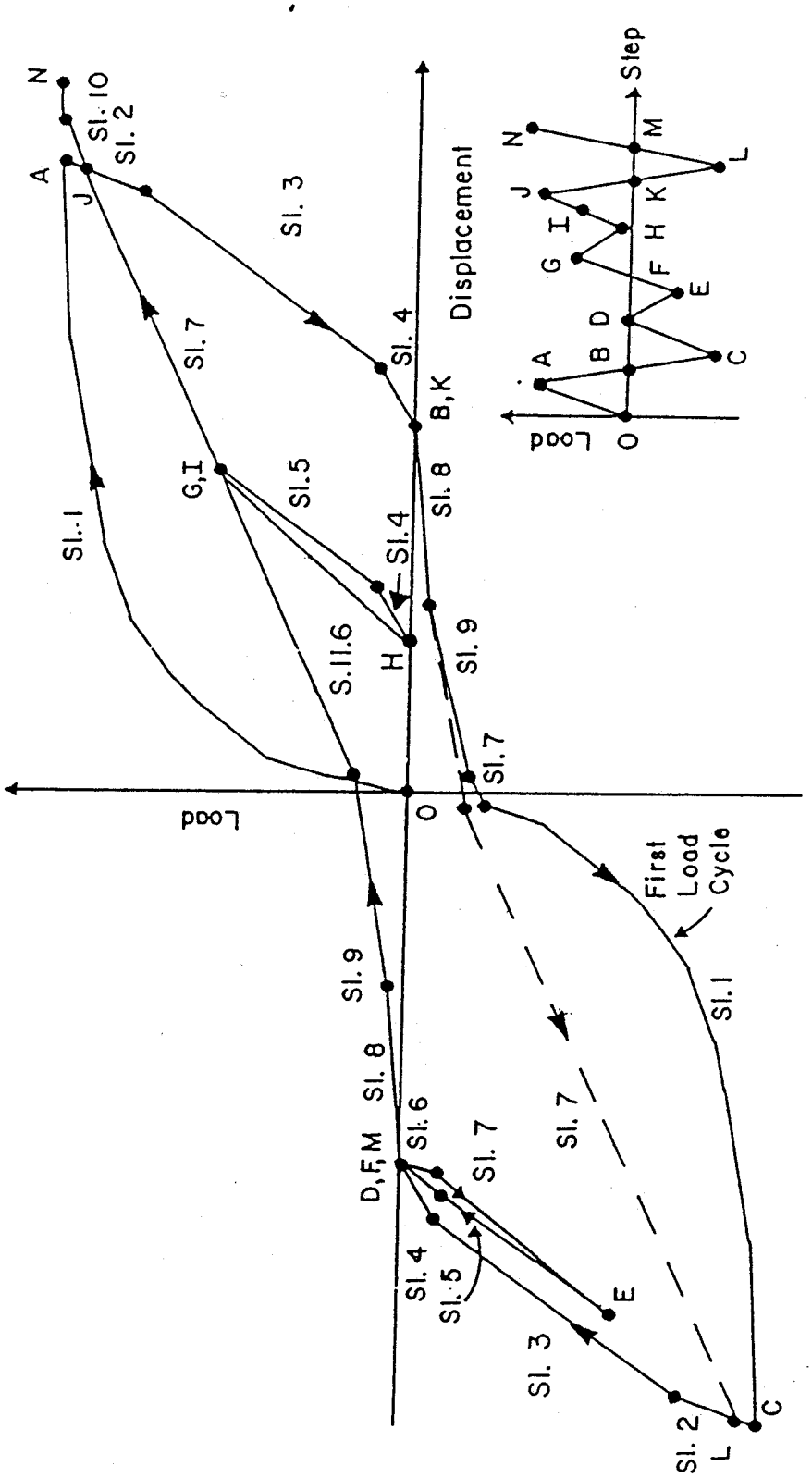

Figure 2.9 Shear Hysteresis Model [5]

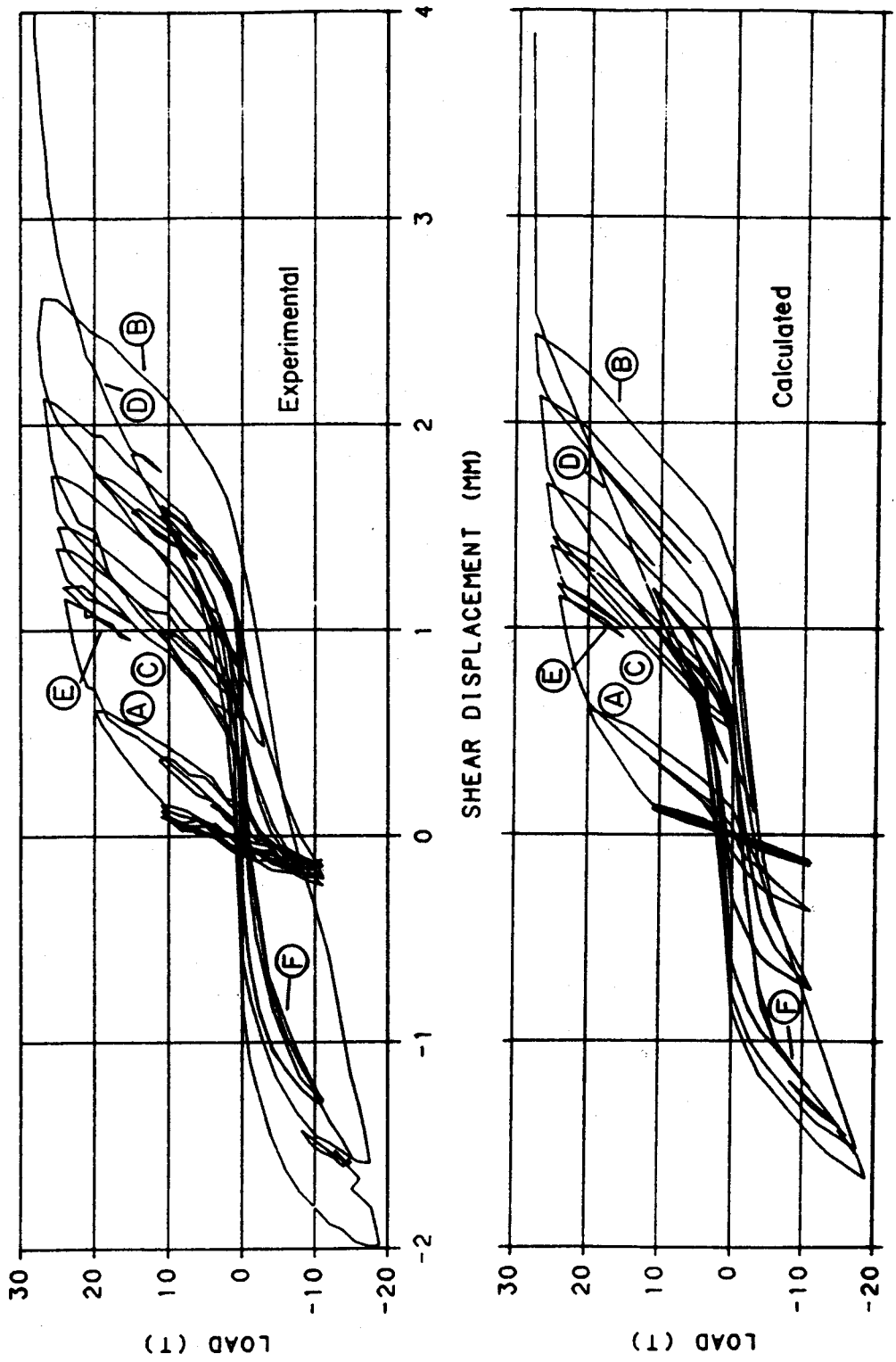

Figure 2.10 Comparison of Calculated and Experimental Shear Hysteresis Loops for NCKU Wall SW-6 [5]

Note: The load is given in metric tons, 1 Ton=2200 lbs.

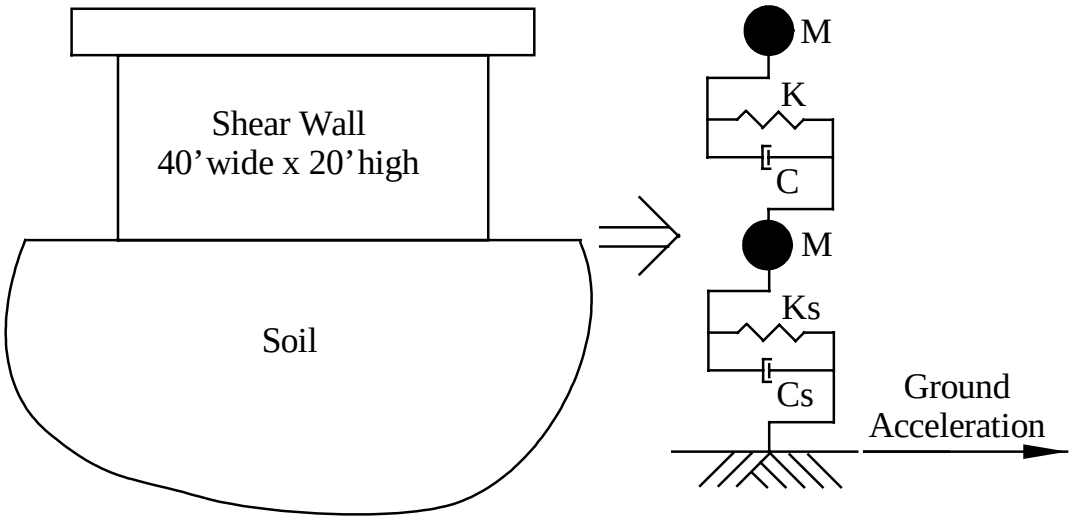

Figure 2.11 SSI Structure

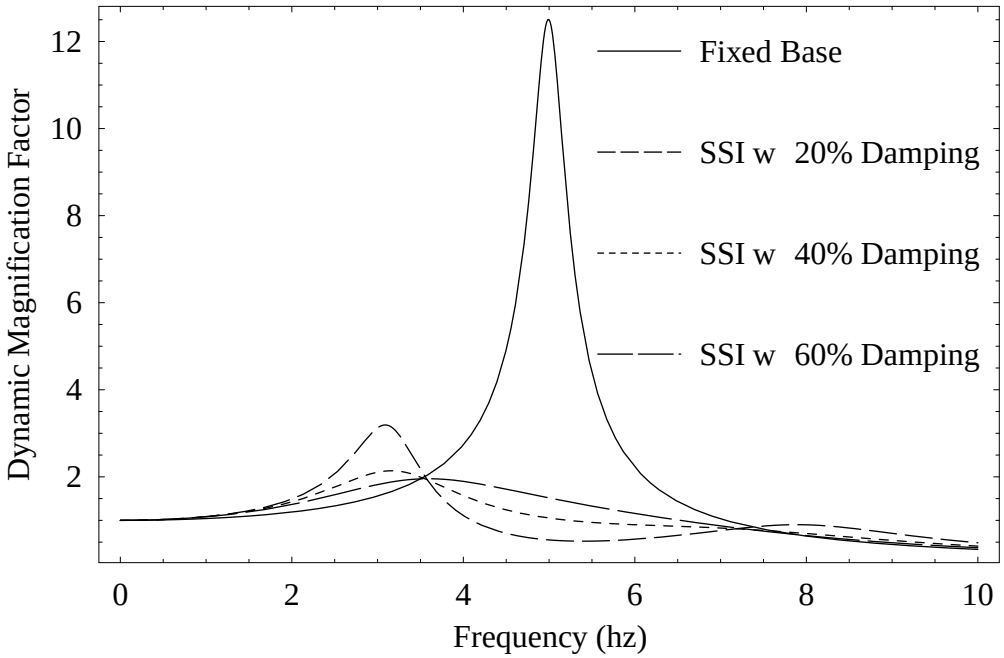

Figure 2.12 5 hz Structural Model – Elastic Sine Sweep

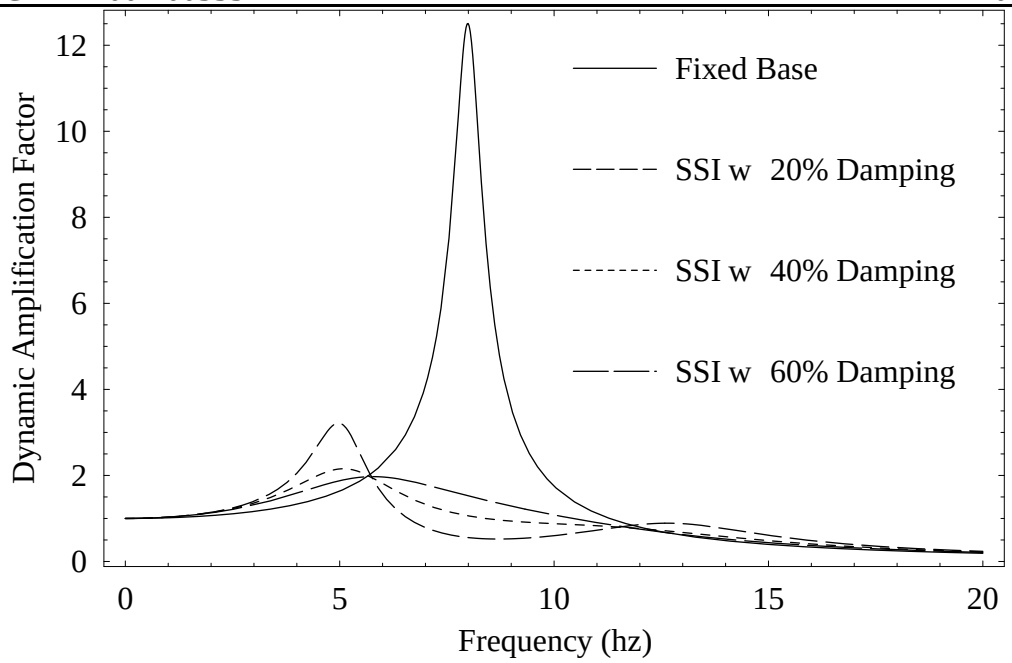

Figure 2.13 8 hz Structural Model – Elastic Sine Sweep

3.0 Discussion of Results

3.1 Fμ For Various Shear Strains

Inelastic force reduction factors, Fμ, are plotted versus peak shear strain in Figures 3.1 and 3.2 for various levels of ground acceleration. In Figure 3.1 the 5 hz fixed base structure is evaluated with different levels of ground acceleration resulting in various combinations of wall shear (demand) and shear strain (limit state). Fμ is calculated for the 5 hz fixed base structure by dividing the elastic demand (wall shear) for a given earthquake by the nonlinear demand due to the same earthquake. Also shown in Figure 3.1 is the response of the same 5 hz structure on soil springs with different magnitudes of soil damping. Fμ for each SSI structure is similarly calculated by dividing the elastic SSI demand (wall shear) for a given earthquake by the nonlinear SSI demand due to the same earthquake.

The data in Figure 3.1 shows that Fμ generally increases with limit state.

Secondly, Fμ in Figure 3.1 decreases for the SSI case as soil damping is increased. Recall the acceleration spectrum in Figure 2.4 is relatively constant between 2 and 8 hz, thus the reduction in Fμ is not due to large differences in ground motion. The cause of this reduction in Fμ is developed below.

The values of Fμ proposed for the draft standard [1] at Limit States A, B and C, Table 3.1, are also shown in Figure 3.1 to be smaller than all of the Fμ calculated for the 5 hz structural model.

Table 3.1 Proposed Fμ For Shear Dominated Shear Walls [1]

Limit State	Fμ	Shear Strain	Fμ Reduced for Weak/Soft Story Effects
LS-A	2.0	0.0075	1.33
LS-B	1.75	0.006	1.24
LS-C	1.50	0.004	1.17

An 8 hz fixed base structure is similarly evaluated in Figure 3.2 with results similar to the 5 hz structure. An important difference is that, overall, Fμ for the 8 hz structure is lower than the 5 hz structure. The reduction in Fμ with increasing frequency for structures in the constant acceleration range with elasto-plastic and bilinear hysteresis behavior was demonstrated by Miranda [7] and others.

The values of Fμ proposed for the draft standard are also shown in Figure 3.2 to be close to the mean calculated Fμ for the 8 hz structural model with SSI having 40% and 60% soil damping.

Overall, the values of Fμ proposed for the draft standard are conservative when compared to the calculated Fμ in Figures 3.1 and 3.2.

The draft standard provides a conservative approach to reduce Fμ to account for the concentration of damage in a weak or soft story. Fμ values calculated using this approach are also provided in Table 3.1. The reduced Fμ are excessively conservative when compared to the calculated values of Fμ. It will be shown in the following section that SSI does not significantly increase damage in a shear wall, thus the weak or soft story Fμ reduction is not applicable.

3.2 Influence of SSI on Wall Damage

The maximum wall shear strain is plotted versus the input ground acceleration in Figures 3.3 and 3.4 for the 5 hz and 8 hz structural models. Note that for a given input ground acceleration the wall shear strain for the fixed base and SSI models is similar. Thus, for the combinations of structural and SSI frequencies examined in this study, SSI does not significantly increase the shear wall damage.

This point is reinforced by comparing the hysteresis loops for the 8 hz fixed base structure and the same structure on soil springs with 60% soil damping in Figures 3.5 and 3.6. Both structures are subject to 0.645 times the input time history. Note that both hysteresis loops have approximately the same number and magnitude of large amplitude loops even though there are some variances in the small amplitude loops.

Wall shear strain time histories for these two walls are compared in Figure 3.7. Note that the frequency content for these two walls is similar but that the peak responses occur at different times. Additionally, the fixed base structure has a larger permanent deformation at the end of the time history than the SSI structure.

The frequency content of the time history in Figure 3.7 can be estimated by counting the number of peaks per second which yields a frequency in the strong amplitude portion of the response of between 1.8 and 2 hz. This represents a reduction in natural frequency by a factor of four and a reduction in effective stiffness by a factor of 16. Recalling that the initial stiffness of the shear wall is 48952 kip/in and the secant stiffness at the 0.0075 strain is calculated by

$$Pc = 6\sqrt{4000}Ag = 3280 \text{ kip}$$

$$Dc = 0.0075\ H = 1.8\text{in}$$

$$K_{\text{Secant @ Ultimate}} = \frac{Pc}{Dc} = 1822\ \frac{\text{kip}}{\text{in}}$$

which is about $^1/_{25}{}^{\text{th}}$ of the elastic stiffness. As seen by the slope of the hysteresis loops, Figures 3.5 and 3.6, the actual stiffness varies from about one-half of the elastic stiffness to much less than the secant stiffness. Thus, the reduction in natural frequency from 8 hz to 2 hz seems reasonable.

The primary reason that SSI did not have a significant influence on damage in Figures 3.3 and 3.4 is because the response of both the fixed base and SSI structures are dominated by the wall's displacement.

The ratio of the wall's peak displacement relative to the peak soil spring displacement can be observed in Figure 3.8. At shear strains between 0.004 to 0.0075 in/in the wall displacements are 10 times, or larger, than the soil displacement and SSI has little effect on response. For the uncracked structure with very low shear strains the soil displacement is actually larger than the wall displacement and SSI has a significant effect on response. Between cracking and low shear strains, say 0.001 in/in, the wall displacements rapidly increase from less than the soil displacement to more than 4 times the soil displacement and the influence of SSI on response rapidly decreases as shear strains increase.

Soil springs do not represent strains in the free-field soil column, nor do they represent the absolute displacement of the free field shown in Figure 2.3. The soil spring displacement represents the relative displacement between the structure and the free-field. If the structure's base has the same displacement as the free-field then the structure behaves as a fixed base.

The stiffness of the soil springs was chosen in this study to shift the SSI frequency to $^{5}/_{8}$ of the fixed base structure frequency. Other values of soil spring stiffness will influence the strain range where SSI ceases to influence the structures response, but, the overall effect will be the same.

3.3 Cause of Fμ Reduction for SSI Systems

One possible cause of the reduction in Fμ observed for SSI structures in Figures 3.1 and 3.2 is the elastic response of the structures. Recall the sine sweep in Figures 2.12 and 2.13 showed that increasing the soil damping reduces the elastic response. Since the shear strains, and corresponding demand, for both fixed base and SSI structures are similar, then it follows that Fμ should also be similar, if the elastic response is similar. Fμ is recalculated in Figures 3.9 and 3.10 by dividing the fixed base elastic demand by the nonlinear demand and is denoted as Fμ'. This eliminates the reduction in elastic force due to SSI damping. The comparison between Fμ' for fixed base and SSI structures has a similar amount of scatter as the shear strain vs ground acceleration plots in Figures 3.3 and 3.4. Thus, the difference in elastic response is the primary reason for the reduction in Fμ for structures with SSI.

Another interpretation of Figures 3.9 and 3.10 is that there is significant conservatism in Fμ for structures which are evaluated with a fixed base analysis.

3.4 Estimated versus Calculated Fμ

Fμ is often estimated for elasto-plastic systems in the constant displacement frequency range as $F\mu = \mu$ based on the equal displacements of elastic and nonlinear structures. Similarly, Fμ is estimated for elasto-plastic systems in the constant acceleration

frequency range as $F\mu = \sqrt{2\mu - 1}$ based on the equal energy of elastic and nonlinear systems.

These two concepts, equal displacements and equal energy are used with the backbone curve in Figure 2.7 to estimate Fμ for a shear wall structure. Estimated Fμ based on equal displacements are developed in Table 3.2 and are shown to be much larger than the calculated Fμ in Figures 3.1 and 3.2. Clearly, the equal displacement approach doesn't apply to this problem.

Table 3.2 Estimated Fμ Based On Equal Displacements Of Elastic And Nonlinear Structures

Shear Strain, γ	Nonlinear Normalized Shear Stress @ γ ($\sqrt{psi}$)	Elastic Normalized Shear Stress @ γ ($\sqrt{psi}$)	$F\mu = \frac{Elastic\,Stress}{Nonlinear\,Stress}$
0.002	5.08	43.	8.5
0.004	5.90	86.	14.6
0.006	6.18	129.	20.9
0.0075	6.22	161.3	25.9

Estimates of Fμ based on equal energy are developed in Table 3.3. For low strains these estimated Fμ are within the range of calculated Fμ. At larger strain levels, the estimated Fμ are larger than the calculated values. Pinching of the hysteresis loops reduces the energy dissipation at larger strain levels and is not accounted for in the estimated Fμ. Reducing the area under the curve to account for pinching would result in a closer agreement between estimated and calculated values at high strains.

Table 3.3 Estimated Fμ Based on Equal Energy Of Elastic And Nonlinear Structures

Shear Strain, γ	Area Under Normalized Backbone Curve ($\sqrt{psi}\,\frac{in}{in}$)	Area Equivalent Elastic Normalized Shear Stress ($\sqrt{psi}$)	$F\mu = \frac{Elastic\,Stress}{Nonlinear\,Stress}$
0.002	0.0013519	9.2	1.8
0.004	0.0118798	23.4	3.9
0.006	0.0240652	32.7	5.3
0.0075	0.0335042	38.5	6.2

3.5 Influence of Elastic Structure Damping on Fμ

The draft standard [1] allows the use of up to 10% damping for the elastic analysis of reinforced concrete structures, which reduces the elastic response but not the nonlinear response. The elastic response is recalculated with 10% damping by scaling the

structural dashpots in Table 2.4 by $^{10\%}/_{4\%}$. The resulting Fμ are shown in Figures 3.11 and 3.12.

The reduction in Fμ from Figures 3.1 and 3.2 to Figures 3.11 and 3.12 is solely due to increasing the damping in the elastic analysis from 4% to 10%. Increasing the fixed base structures damping directly reduces the fixed base response while increasing the structure damping on the SSI model has a lesser affect because of the large SSI damping.

Overall, the Fμ proposed by the draft standard [1] are conservative compared to the calculated values in Figures 3.11 and 3.12. The Fμ are negligibly unconservative for the 8 hz SSI structure with 40% and 60% soil damping.

3.6 Influence of Nonlinear Structure Damping on Fμ

A constant damping is assumed for the shear wall in this study. The magnitude of the dashpot is determined by

$$C = \rho\, 2\sqrt{K\,M} = \rho\, 4\pi\, fn\, M$$

where ρ is 4%,
K is the initial stiffness,
fn is the initial natural frequency, and
M is the mass.

As the structure deforms nonlinearly, the stiffness and effective frequency, fe, decrease. Since the damping value is held constant, then the effective damping ratio, ρe, increases by

$$\rho e = \rho \frac{fn}{fe}$$

and the nonlinear structure can have significantly more viscous damping than the elastic structure. Mechanistically it is reasonable that a heavily cracked wall would have a higher viscous damping than a very lightly cracked wall. However, data to validate the effective damping used in this study is not readily available.

An undamped 8 hz fixed base structure is evaluated to understand the influence of the damping formulation used in this study. The peak ground acceleration for both damped and undamped structures is shown in Figure 3.13. At a common level of ground acceleration the undamped structure has more damage (strain) than the damped structure. In terms of an energy balance, the damped structure requires less strain energy than the undamped structure because of energy dissipation due to damping. The gap between the damped and undamped curves in Figure 3.13 is larger at high strains than at low strains because the effective damping ratio is larger at low effective frequency or high strains.

Fμ for the undamped and damped structure are shown in Figure 3.14. Fμ for the undamped structure are considerably larger than the damped structure because the undamped wall force is about 2.4 times larger than the 4% damped wall force. If we were to make the overly conservative assumption that elastic structures have 4% damping and nonlinear structures don't have any damping then Fμ can be estimated by dividing the "No Damping" curve in Figure 3.14 by 2.4, which is still consistent with the Fμ proposed in the draft standard.

The damping formulation used in this study is judged to be reasonable because a heavily cracked wall is believed to have a higher viscous damping than a very lightly cracked wall. Figures 3.13 and 3.14 demonstrate that the magnitude of damping does not significantly alter behavior – the data sets have the same trends with different magnitudes. Additionally, Figure 3.14 demonstrates that removing all damping would actually increase Fμ.

3.7 Frequency Content of Structures with Nonlinear Behavior

In-structure elastic response spectra, with 5% damping, are generated for the motion at the top of the shear wall to understand how the effective frequency varies with strain level. Figures 3.15 through 3.18 contain response spectra for the 5 hz fixed base structure and the 3.1 hz SSI structures. Each spectrum represents the response of one nonlinear structure with successively larger input motions. Walls with a peak shear strain greater than 0.0075 are omitted.

As the magnitude of input motion is increased, the frequency of peak response decreases. This phenomena is illustrated in Figure 3.15b which shows the spectra at four different strain levels ranging from incipient cracking to 0.0075 in/in. The frequency of peak spectral acceleration for each response spectra is shown in Figures 3.19 and 3.20 as a function of the peak wall shear strain. The reduction in effective frequency is quite dramatic, especially for larger input motions.

Notice that the nonlinear structures seem to respond at discrete frequencies, even for larger input motions. This is probably due to local peaks and valleys in the input motion's frequency content.

Natural frequencies for SSI structures are determined by an eigensolution which neglects damping. The stiffening effect of damping is evident in Figure 3.19 where, for low input motions, the 3.1 hz SSI structures with 40 and 60% soil damping have an effective frequency of about 3.9 hz. Note that 3.9hz does correspond to a local peak in the input motion and the actual effective frequency for these two structures is a function of damping. This is evident for the 40 and 60% damped structures in Figure 3.20. Elevated natural frequencies for the SSI structures with large damping can also be observed in the sine sweeps in Figures 2.12 and 2.13.

The effective frequencies are divided by their elastic frequency and plotted against peak shear strain in Figures 3.21 for fixed base structures and 3.22 for SSI structures. For the fixed base structures in Figure 3.21 it is evident that significant frequency shifts occur,

even at relatively low shear strains (0.001 in/in). For strains near 0.0075 in/in, which corresponds to Limit State A in the draft standard, the effective frequency is between 19% and 26% of the initial frequency.

The reduction of effective frequency for SSI structures in Figure 3.22 is not as large as the fixed base structures because the SSI initial frequencies are $^5/_8$ of the fixed base frequencies.

The calculated effective frequency for a SDOF structure, based on the approach in NUREG/CR-3805 [9] is also shown in Figure 3.21 and provides a reasonable estimate of the effective frequency. The calculated effective frequency is given by the relationship

$$\frac{f'e}{f} = (1 - A) + A\frac{fs}{f}$$

where fs is the natural frequency based on the secant stiffness at strain ε,
f is the initial stiffness,
$A = Cf\,(1 - \frac{fs}{f}) < 1.0$, and
Cf is 2.7.

The calculated effective frequency for a SDOF structure is used to determine the structure's effective stiffness, which is combined with the soil stiffness and mass to determined the effective frequency for SSI structures. As shown in Figure 3.22, this effective frequency for SSI structures is also a reasonable estimate of the actual effective frequency.

The response spectrum for an elastic structure which meets the acceptance criteria of the draft standard with Fμ=2.0 is also shown in Figures 3.15 through 3.18. The response spectra for the elastic structure overestimates the response and misses the effective frequency. The difference in both frequency and amplitude are more exaggerated for the fixed base structure than for the SSI structure.

3.8 Correlation Between Input Energy and Shear Strain

The correlation between input energy and shear strain is shown in Figure 3.23. Wall damage, in the form of shear strain, is clearly dependant on the input energy. Input energy is the estimated by

$$\text{Input Energy} = \tfrac{1}{2}\,M\,(Sv)^2$$

where M is the structure mass in Table 2.4,
Sv is the effective spectral velocity given by, $Sv = \frac{Sa(fn_{Effective}) \times g}{2\,\pi\,fn_{Effective}}$
g is the acceleration due to gravity,
Sa is the 4% damped spectral acceleration shown in Figure 2.5, and

$fn_{Effective}$ is the effective natural frequency from Figures 3.19 and 3.20.

This correlation could be used to determine the wall shear-strain demand for a given intensity of ground motion and deserves attention in future studies.

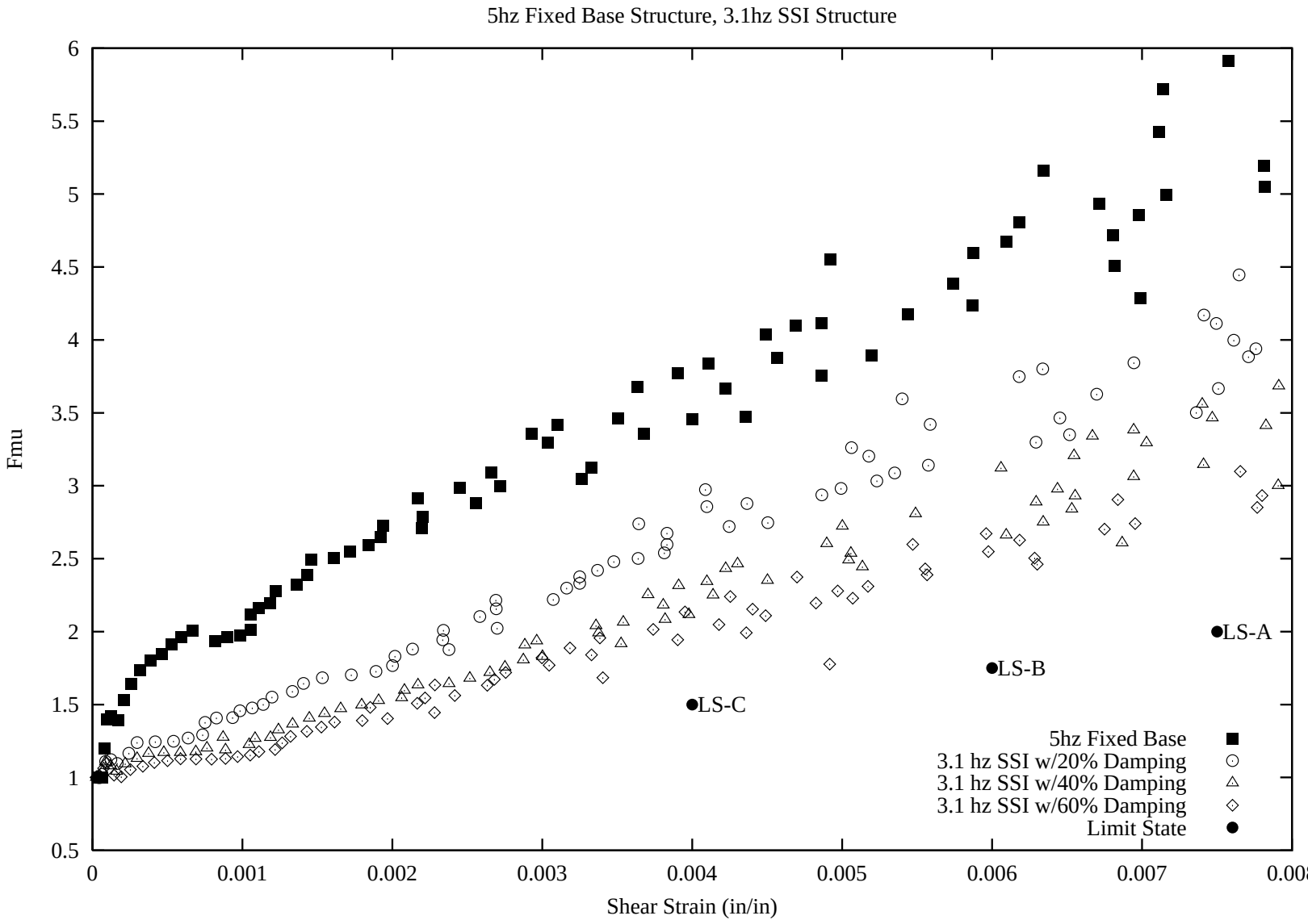

Figure 3.1 Fμ vs Shear Strain for the 5 hz Structural Model

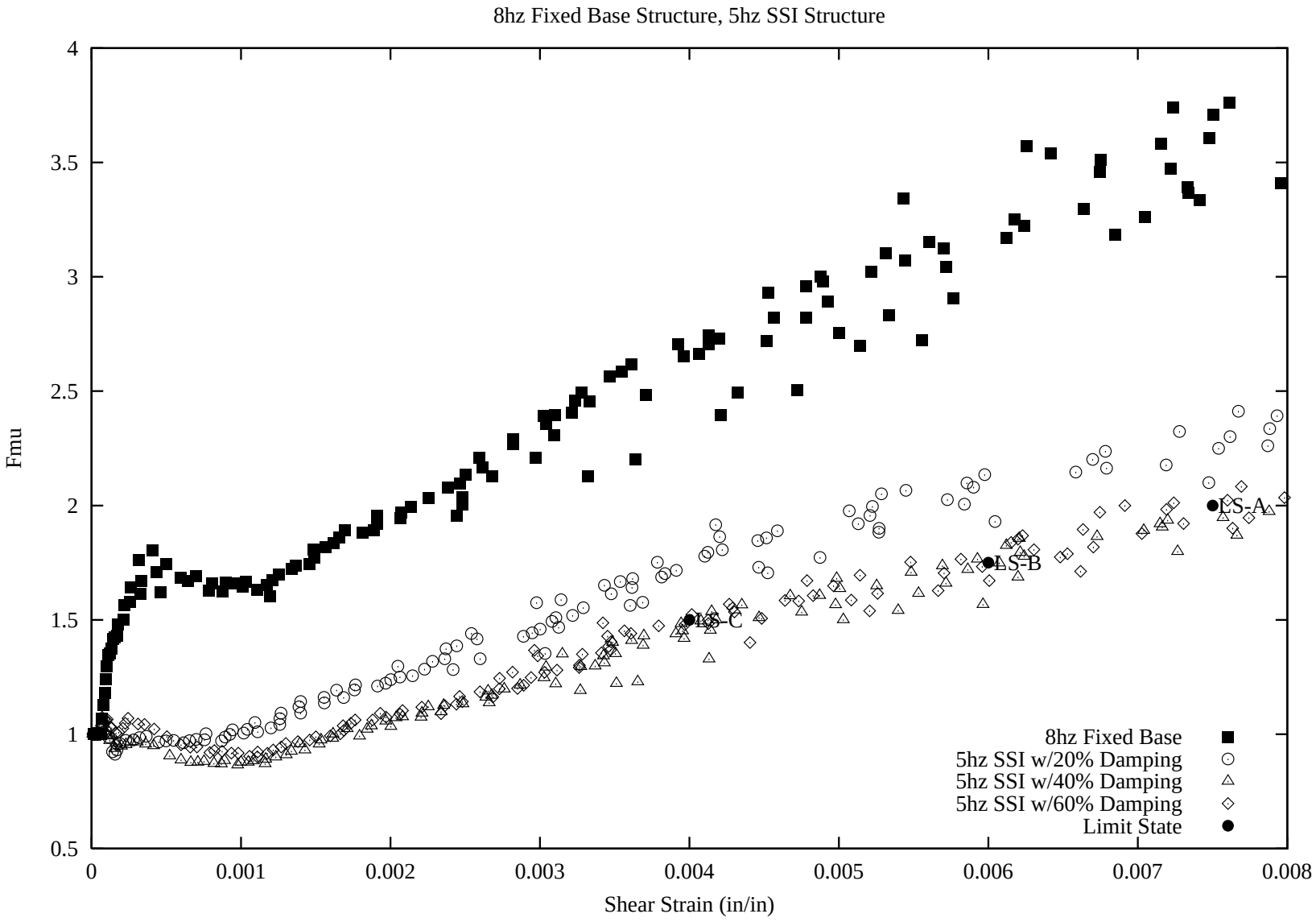

Figure 3.2 Fμ vs Shear Strain for the 8 hz Structural Model

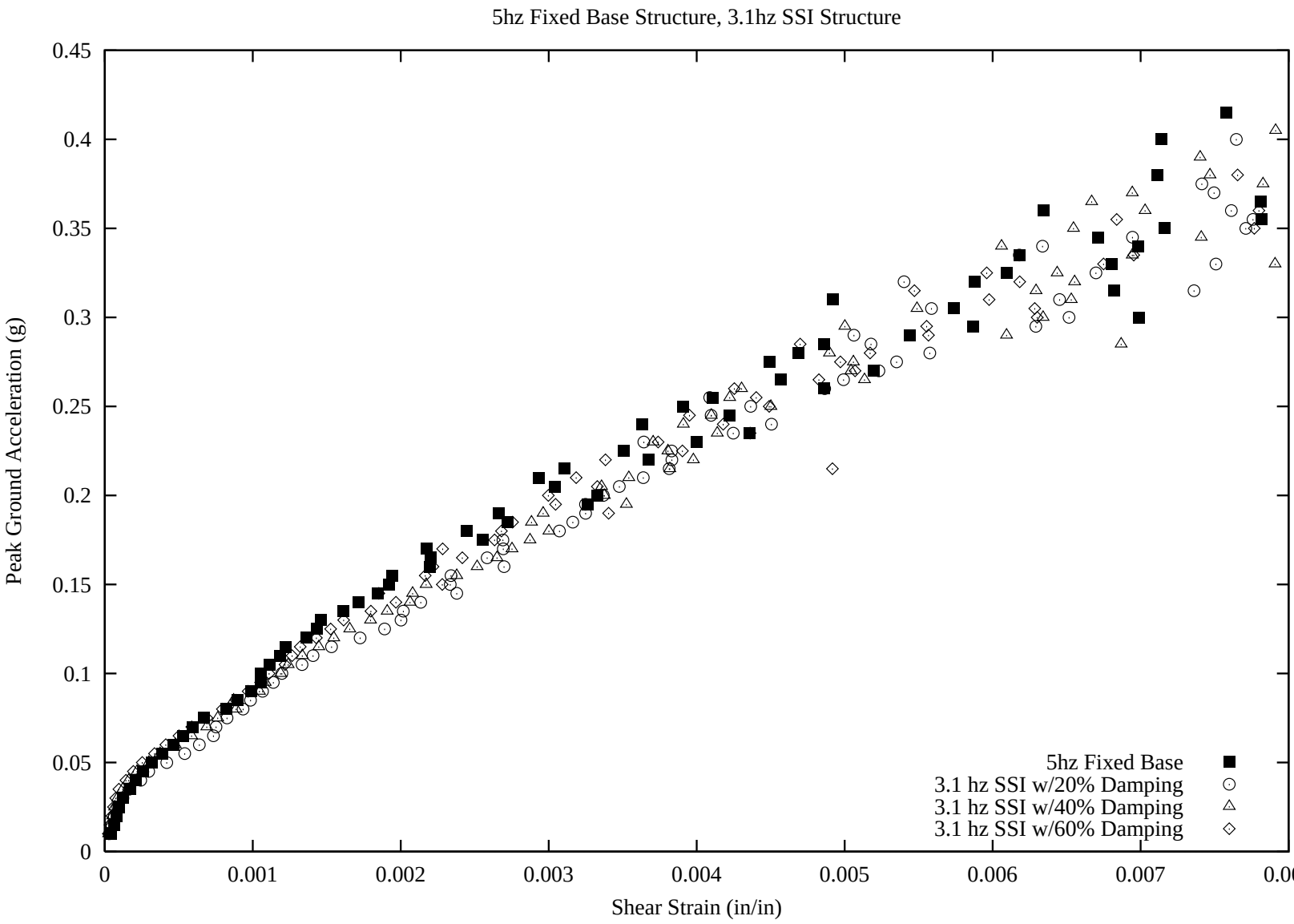

Figure 3.3 Shear Strain vs Peak Ground Acceleration for the 5 hz Structural Model

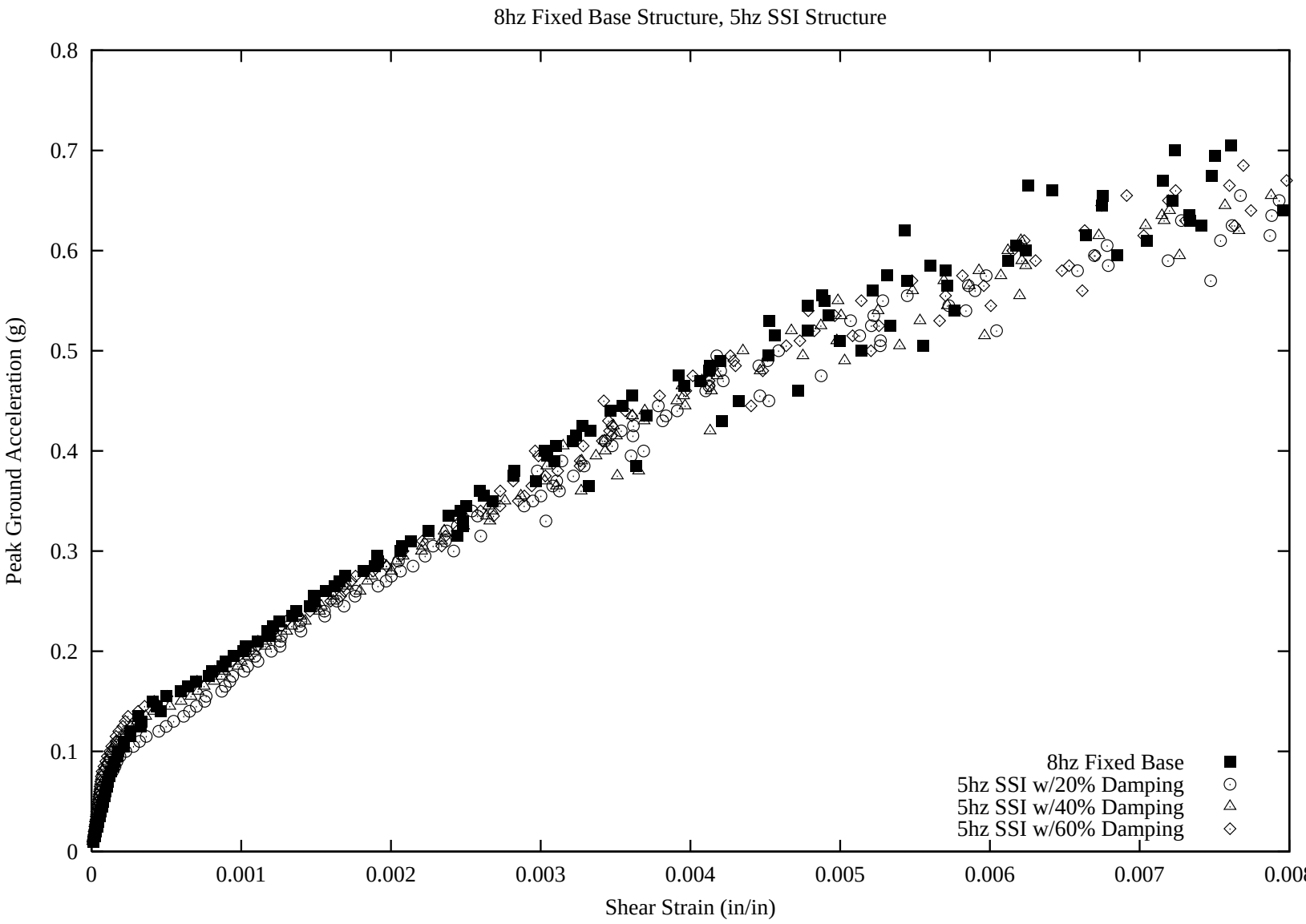

Figure 3.4 Shear Strain vs Peak Ground Acceleration for the 8 hz Structural Model

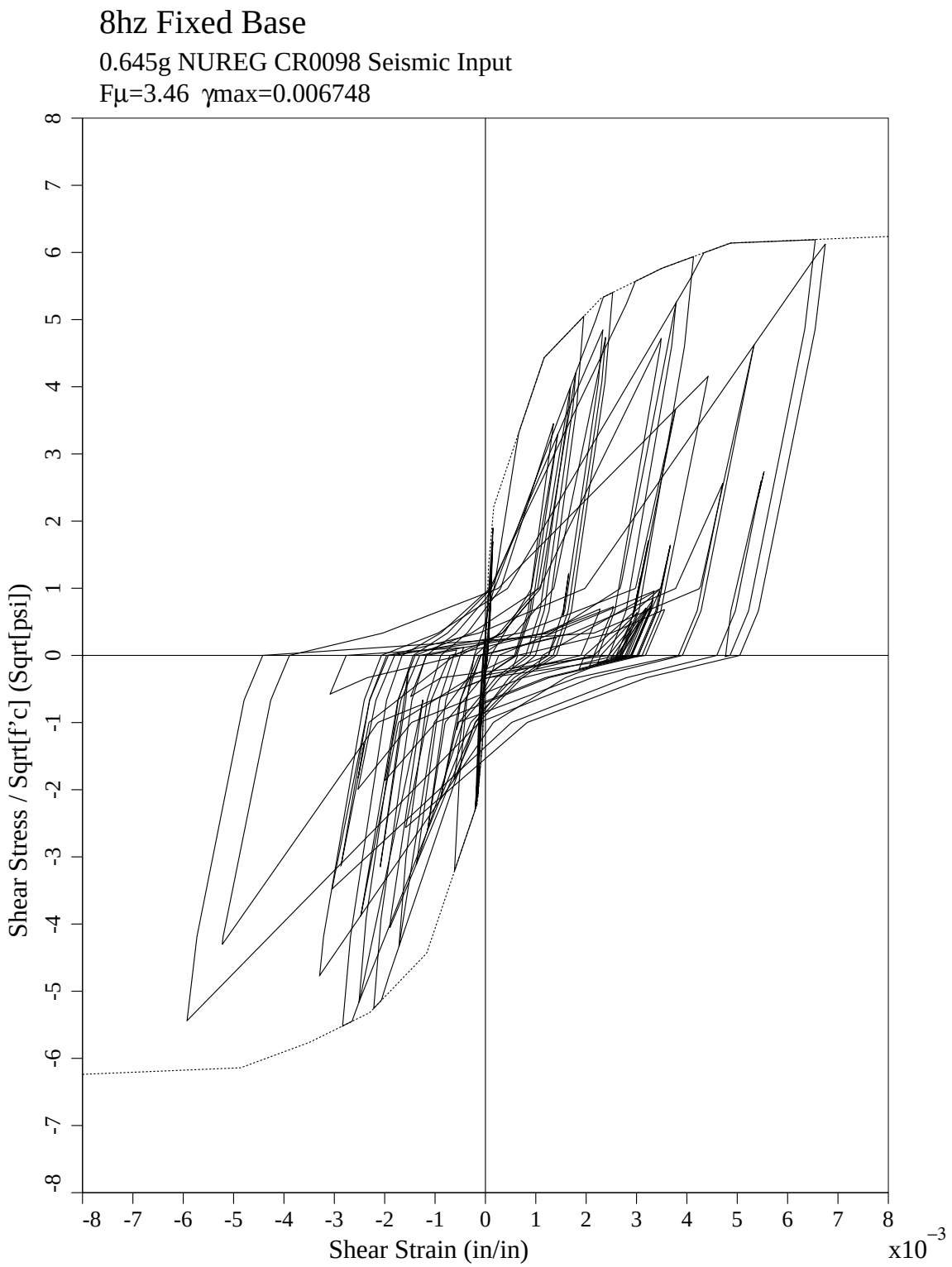

Figure 3.5 Wall Shear Stress-Strain Relationship for the 8 hz Fixed Base Structure At 0.645 x Input Time History

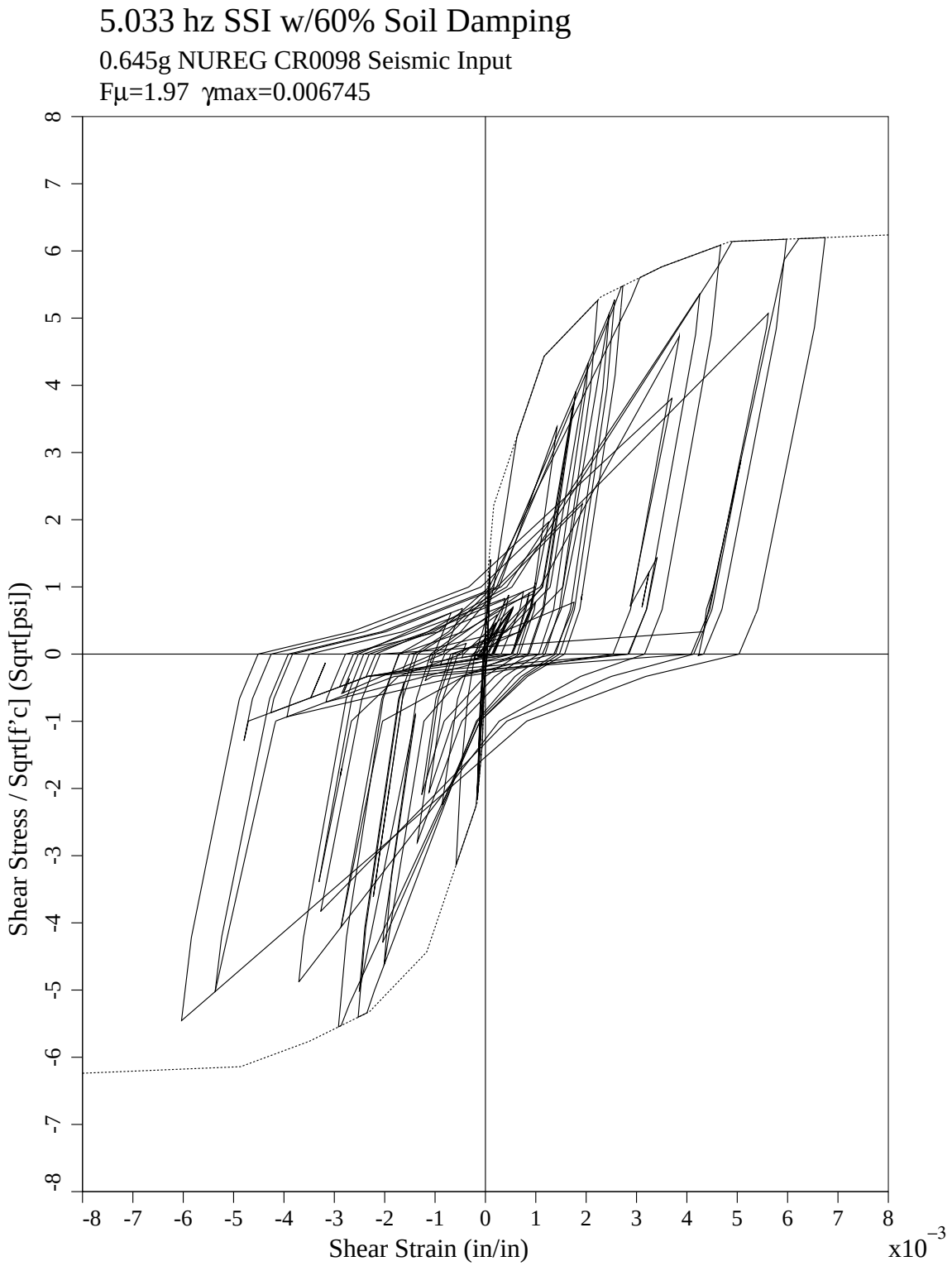

Figure 3.6 Wall Shear Stress-Strain Relationship for the 5 hz SSI Structure with 60% Soil Damping At 0.645 x Input Time History

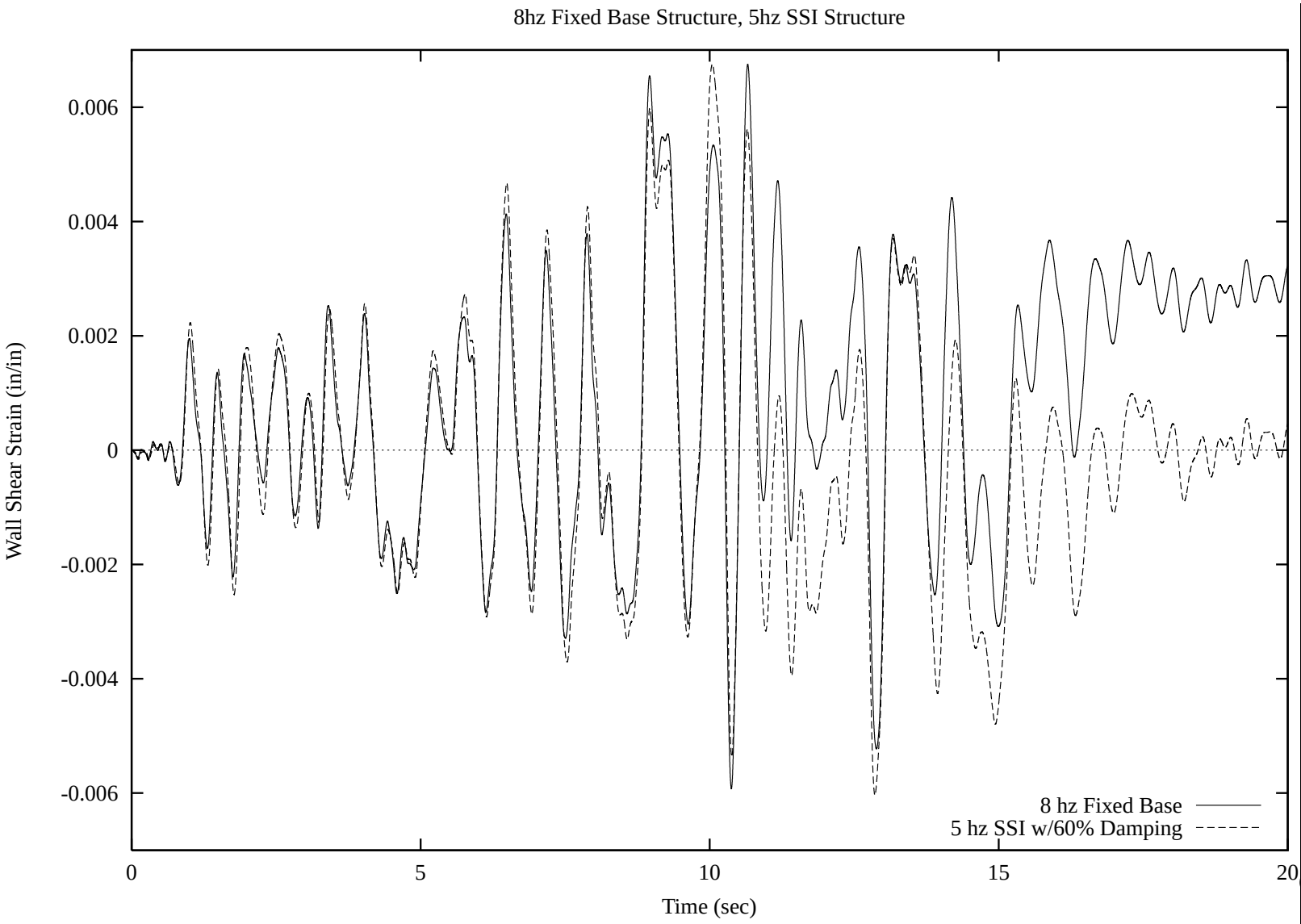

Figure 3.7 Shear Strain Time Histories for 8 hz Fixed Base and 5 hz SSI Structures At 0.645 x Input Time History

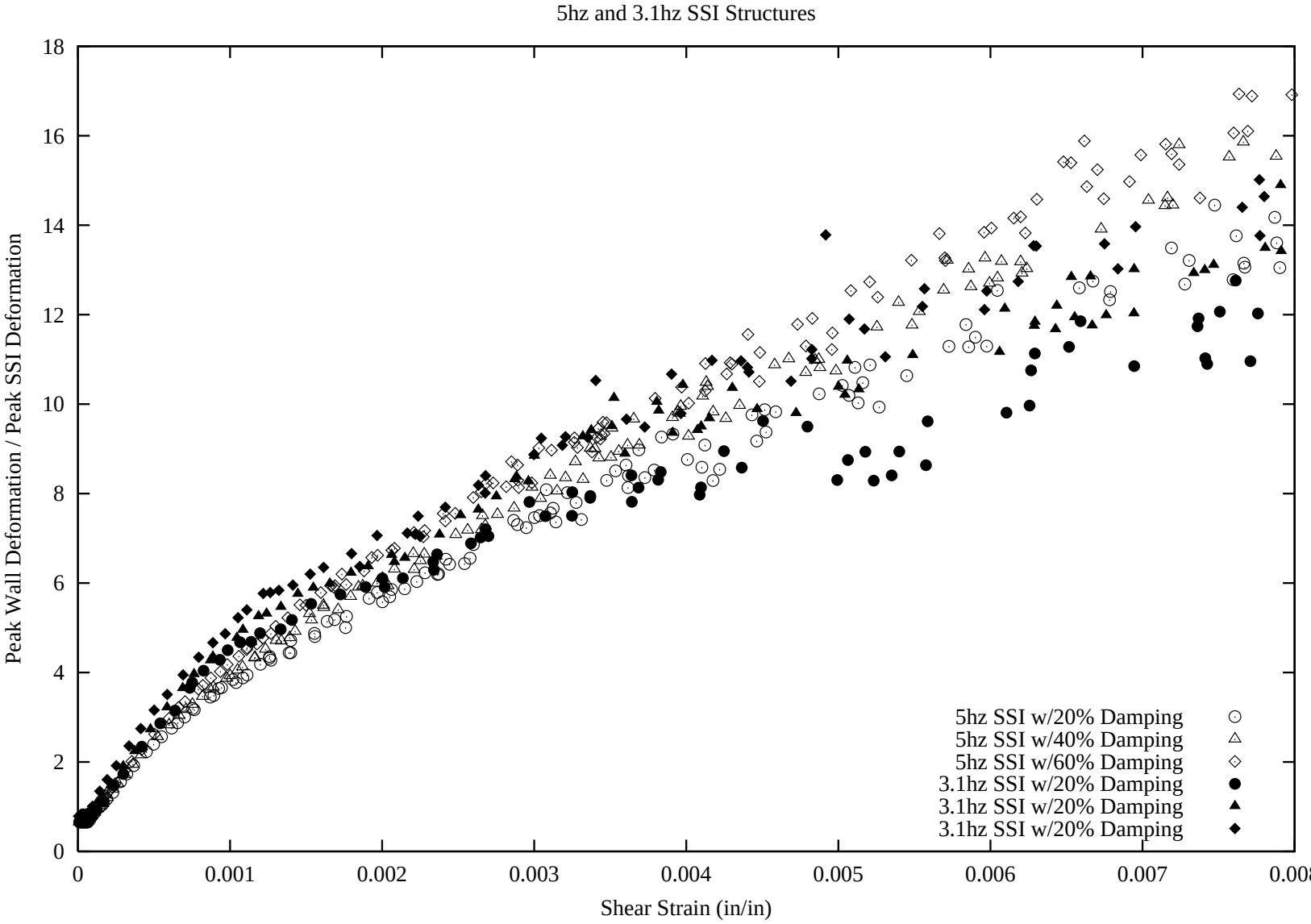

Figure 3.8 Ratio of Shear Wall Displacement to Soil Spring Displacement vs Shear Strain

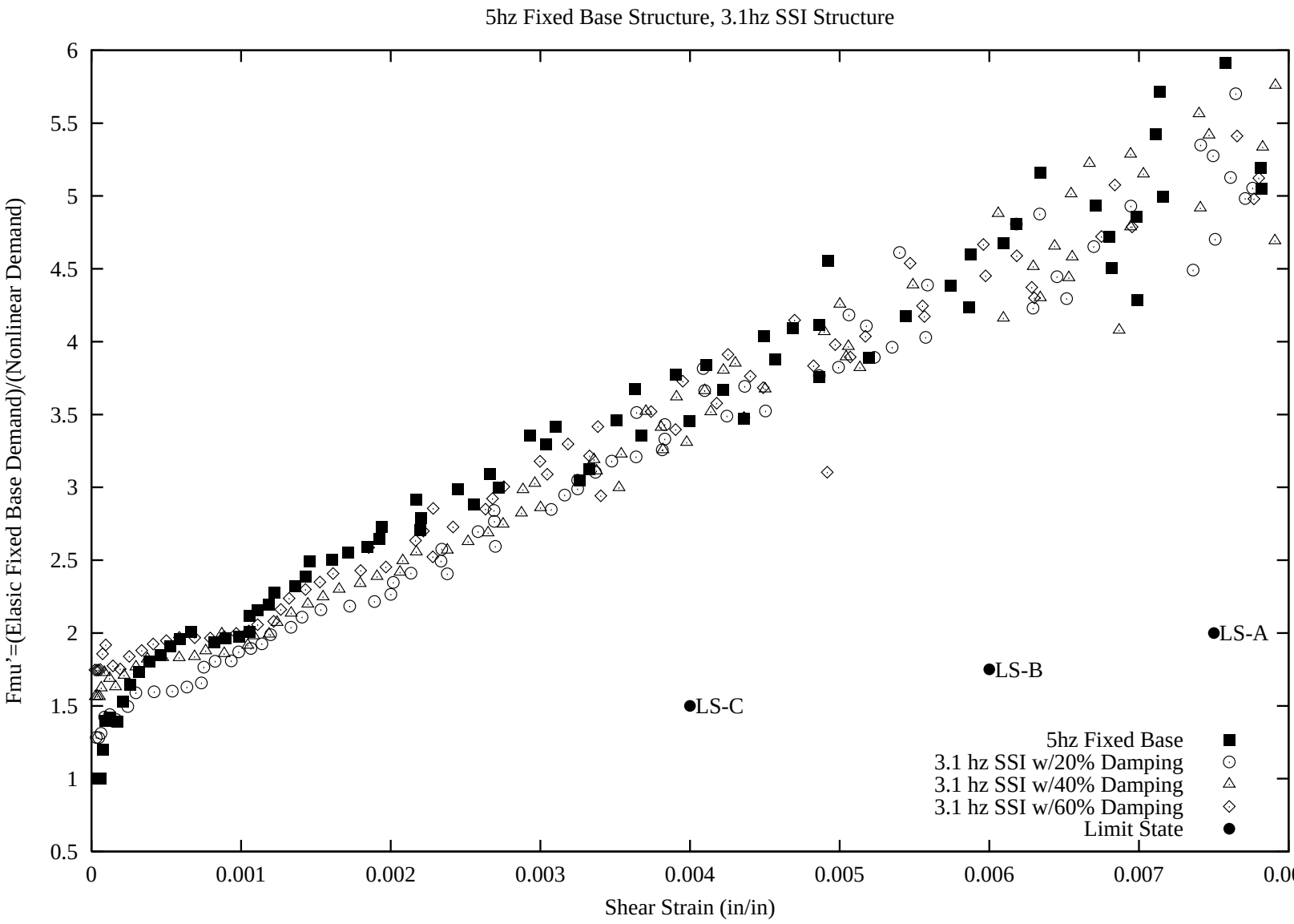

Figure 3.9 Fμ' vs Shear Strain for the 5 hz Structural Models

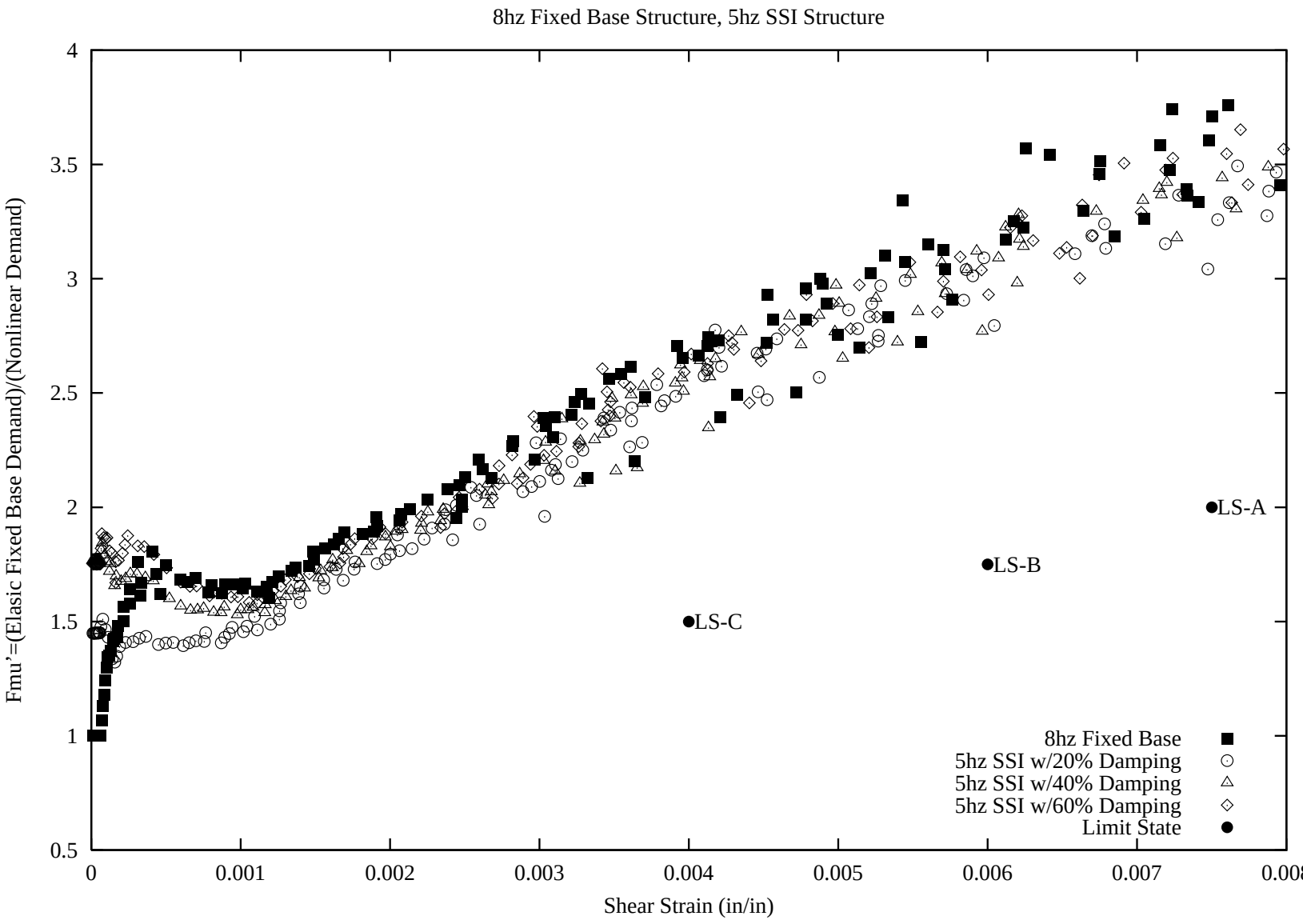

Figure 3.10 Fμ' vs Shear Strain for 8 hz Structural Models

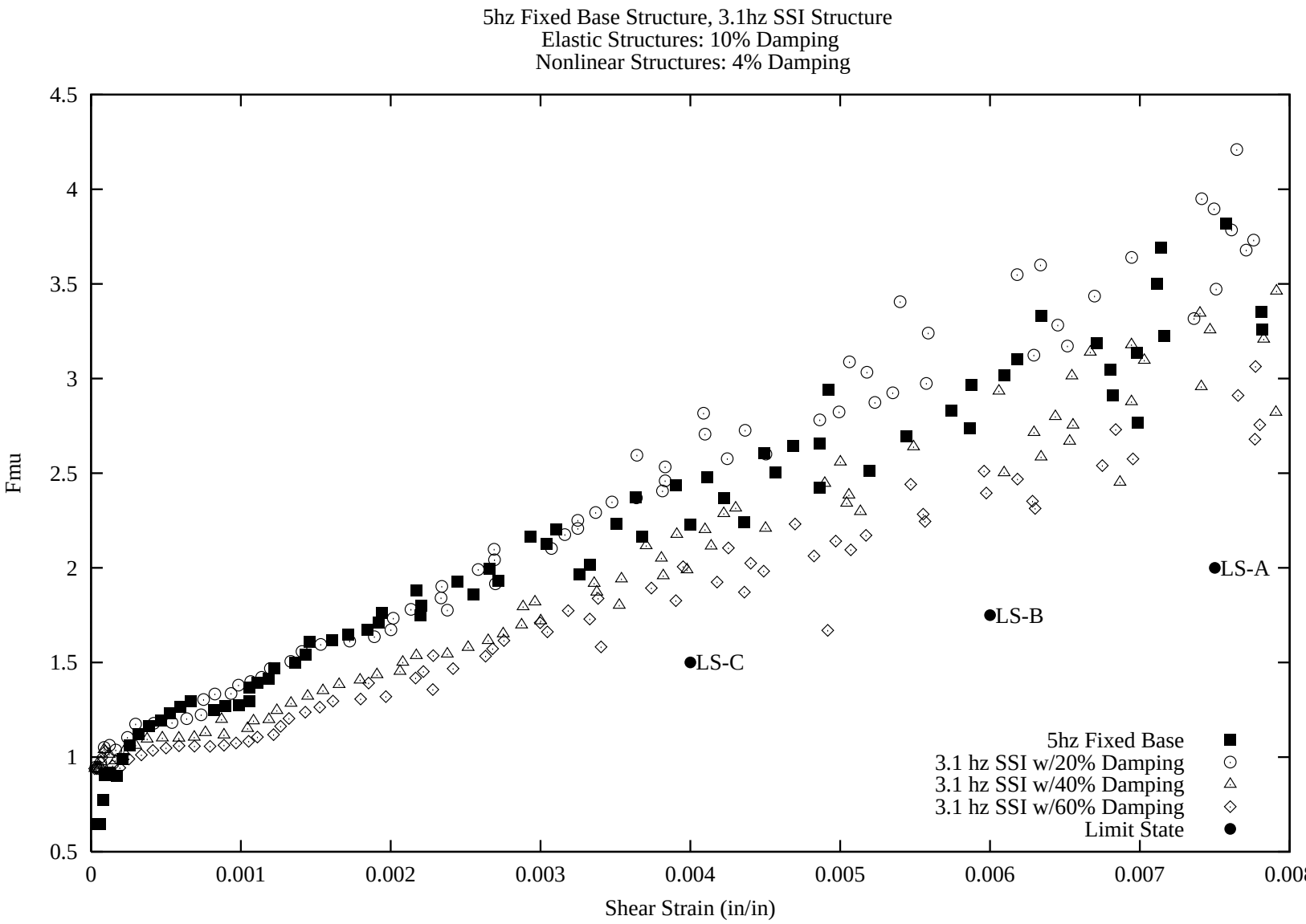

Figure 3.11 Fμ vs Shear Strain for 5 hz Structural Models, Elastic Response Includes 10% Damping

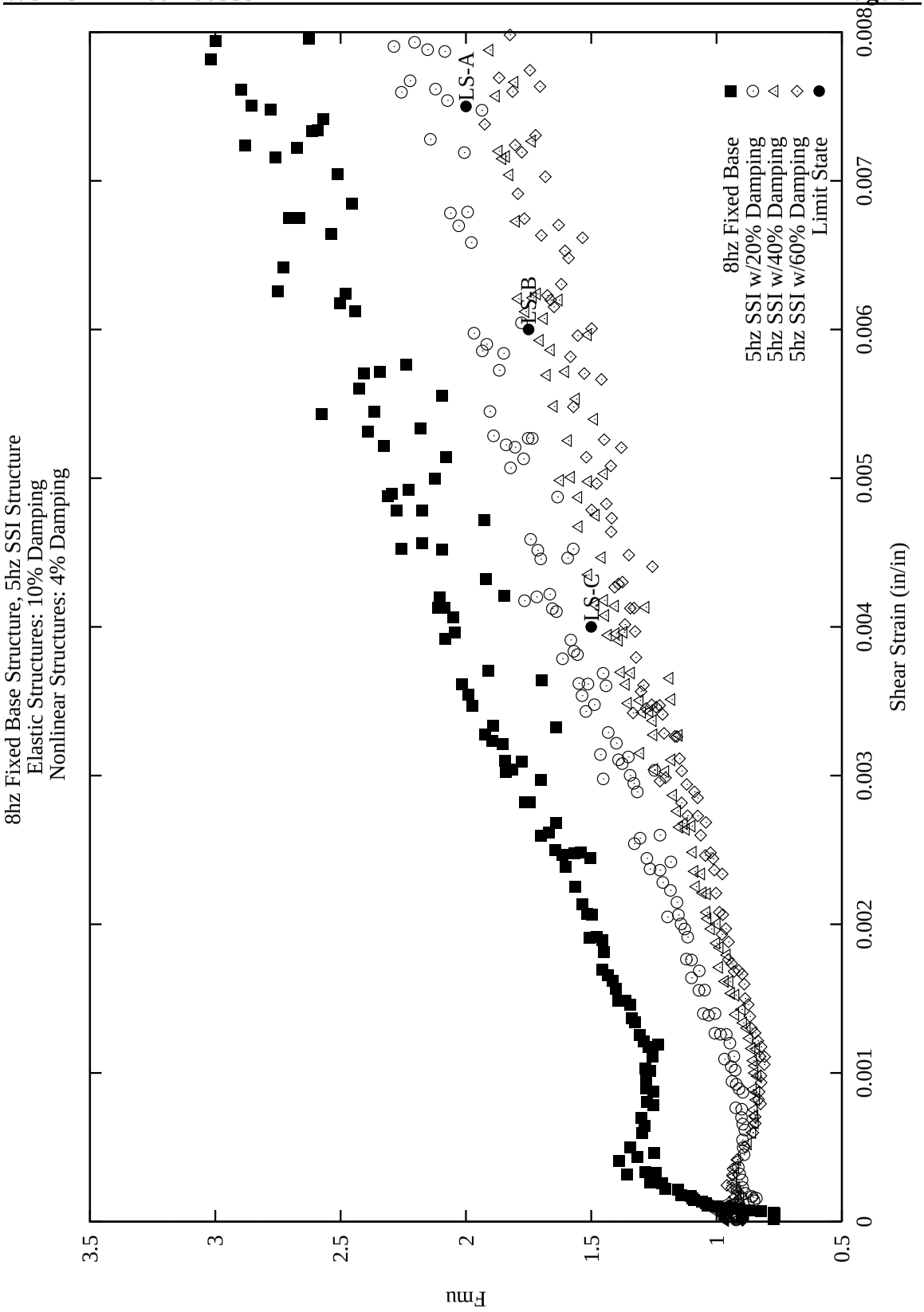

Figure 3.12 Fμ vs Shear Strain for 8 hz Structural Models, Elastic Response Includes 10% Damping

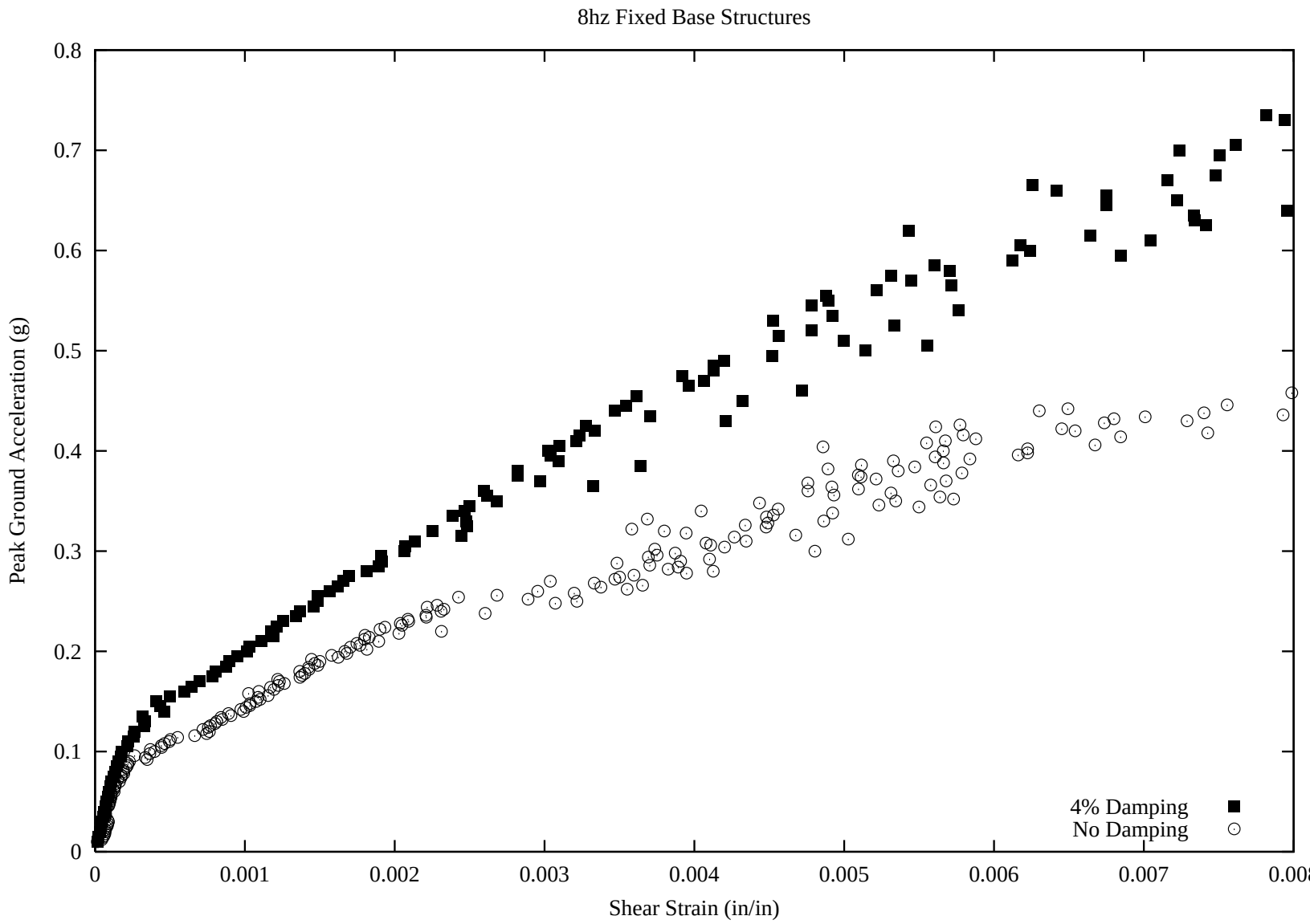

Figure 3.13 Shear Strain vs Peak Ground Acceleration for 8 hz Fixed Base Structures with and without Damping

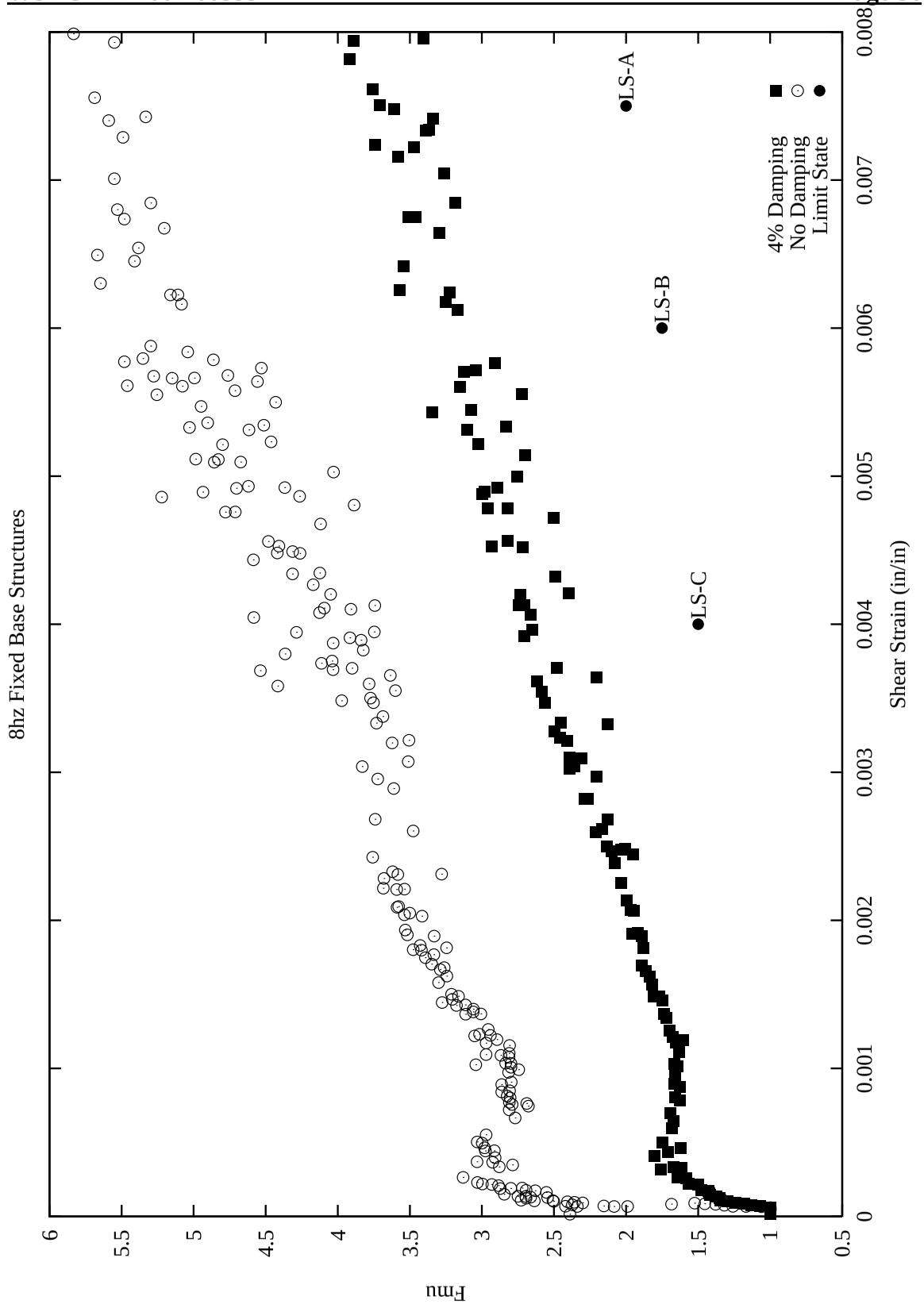

Figure 3.14 Fμ vs Shear Strain for 8 hz Fixed Base Structures with and without Damping

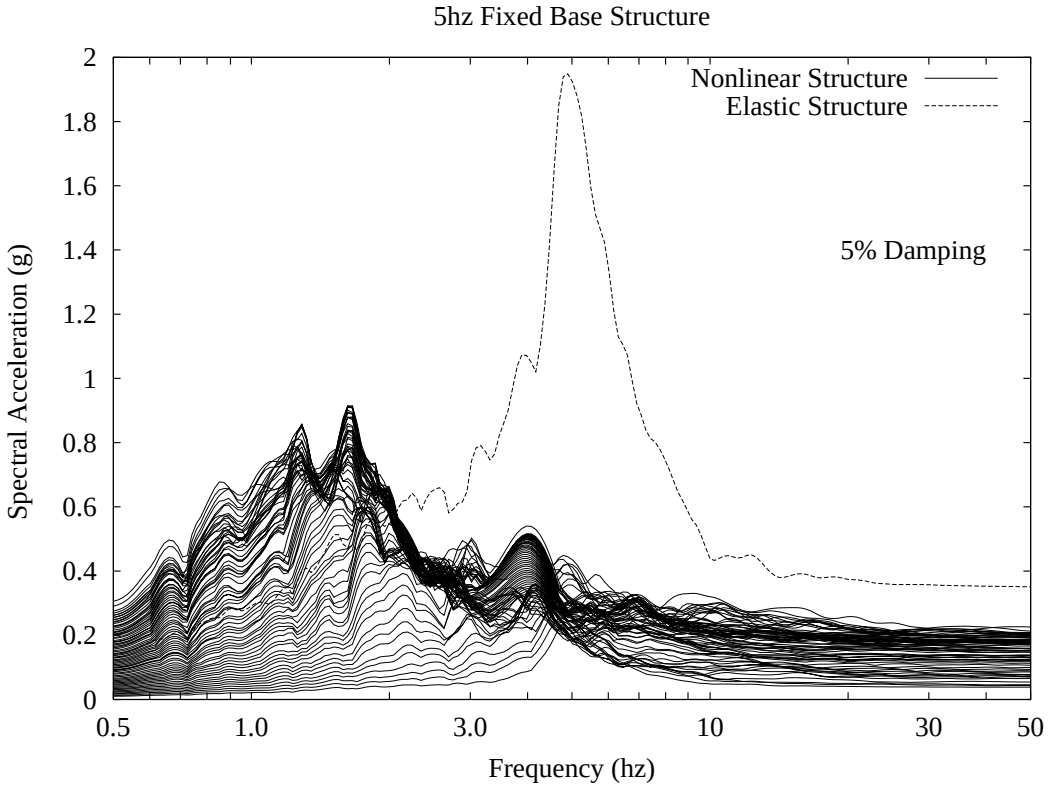

Figure 3.15a In-Structure Response Spectra for 5 hz Fixed Base Structure

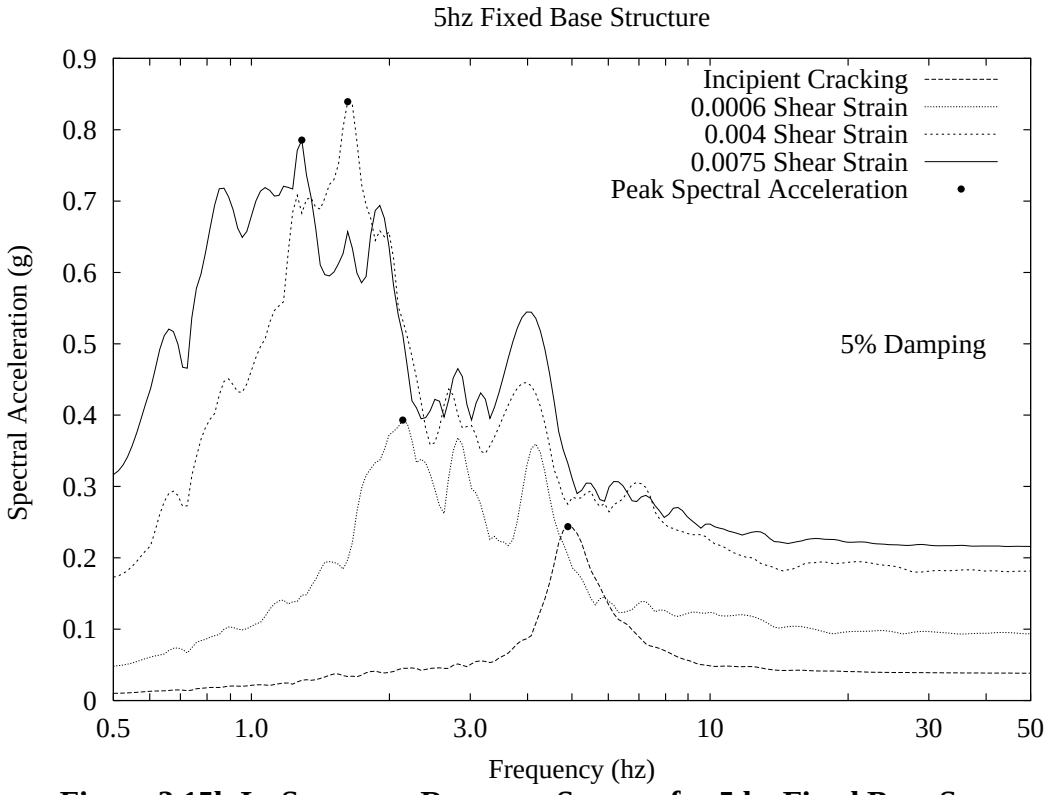

Figure 3.15b In-Structure Response Spectra for 5 hz Fixed Base Structure

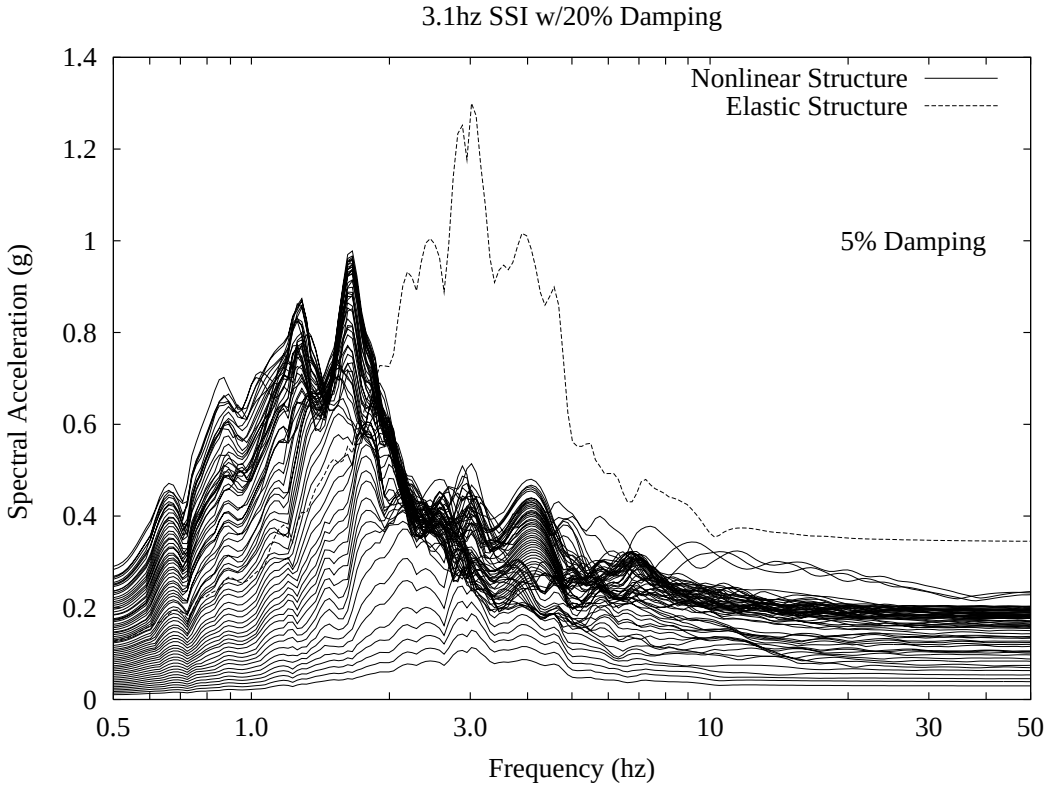

Figure 3.16 In-Structure Response Spectra for 5 hz SSI Structure with 20% Soil Damping

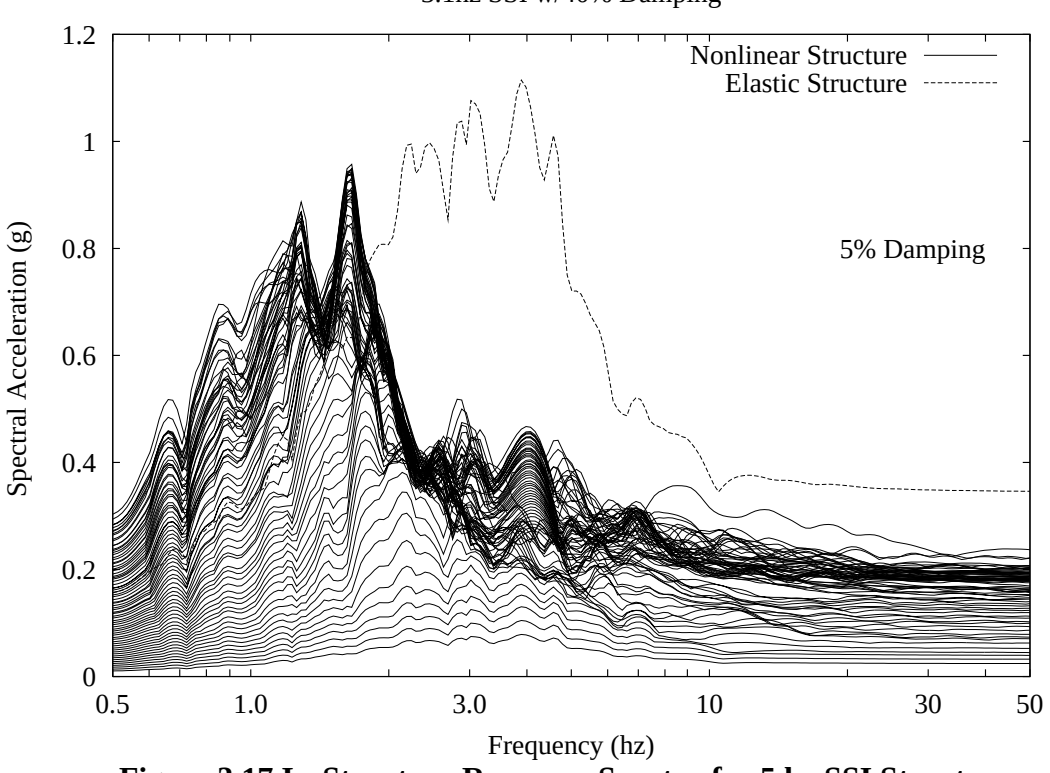

Figure 3.17 In-Structure Response Spectra for 5 hz SSI Structure with 40% Soil Damping

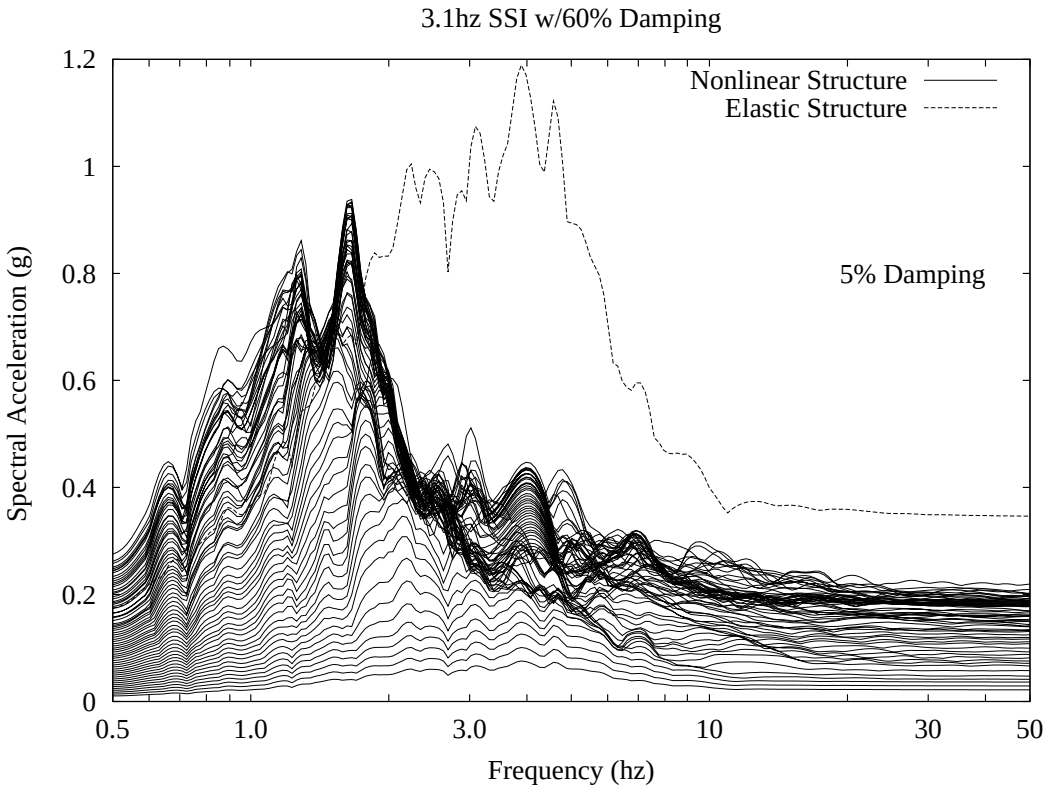

Figure 3.18 In-Structure Response Spectra for 5 hz SSI Structure with 60% Soil Damping

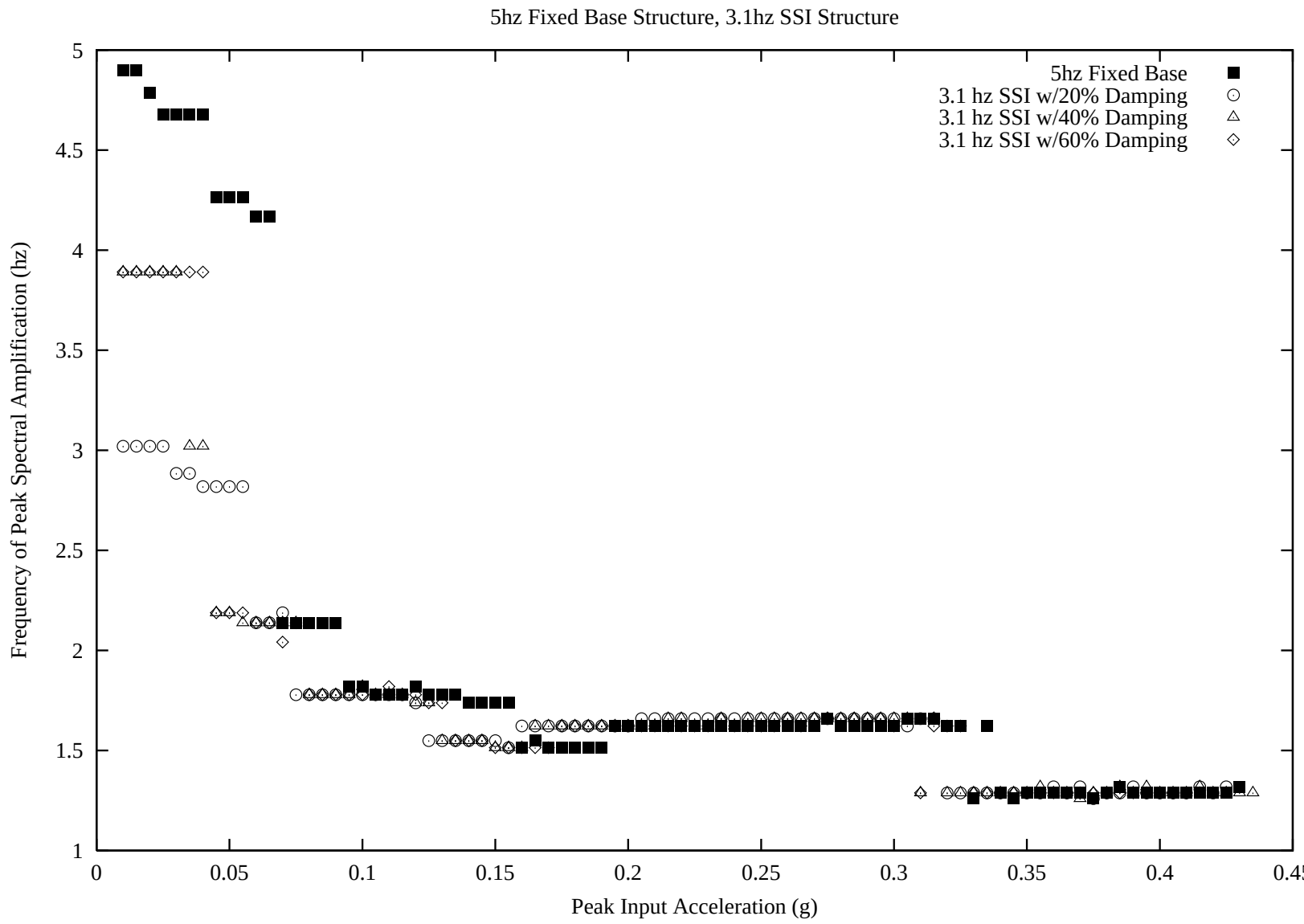

Figure 3.19 Effective Frequency for 5 hz Fixed Base and 3.1 hz SSI Structures

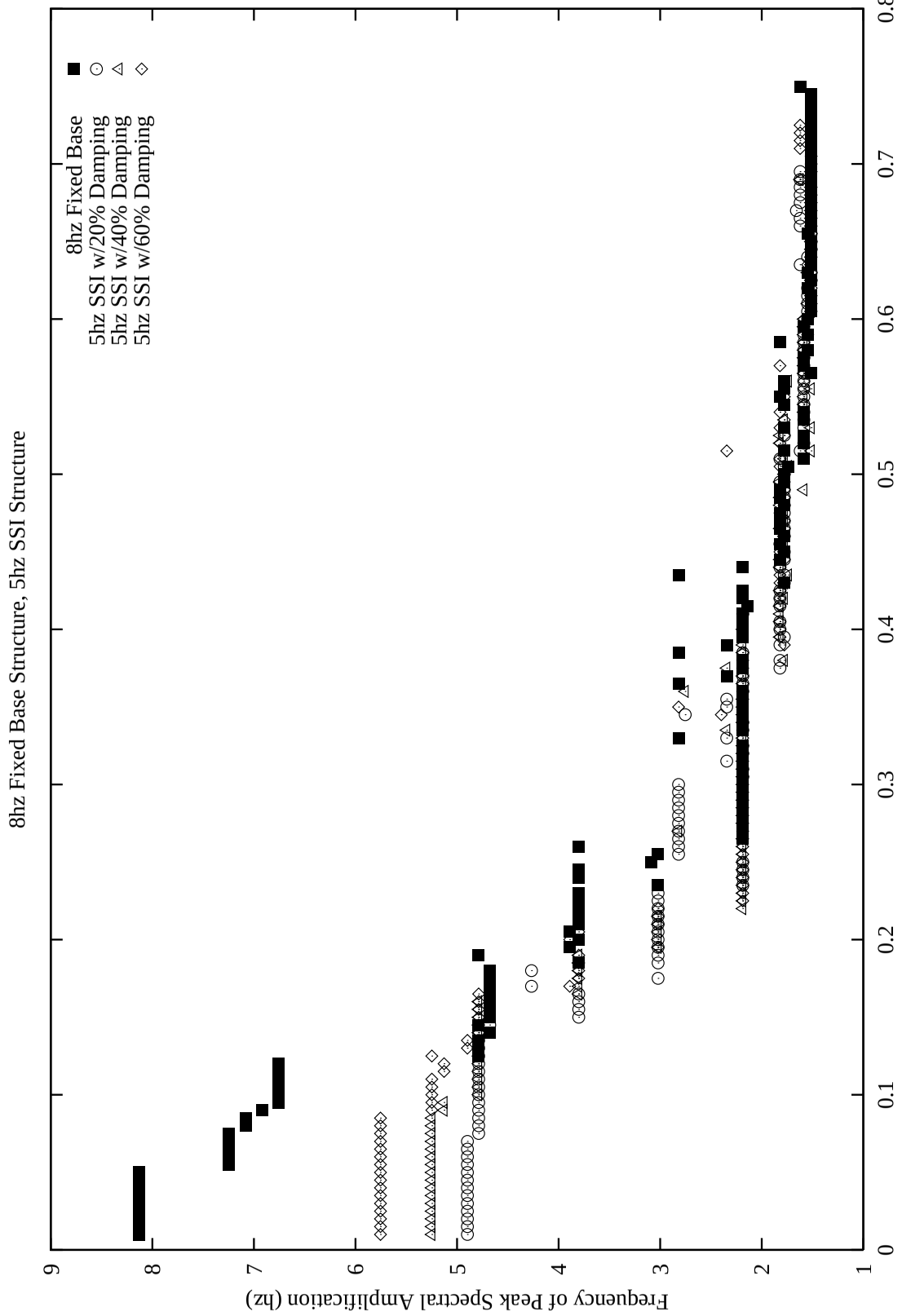

Figure 3.20 Effective Frequency for 8 hz Fixed Base and 5 hz SSI Structures

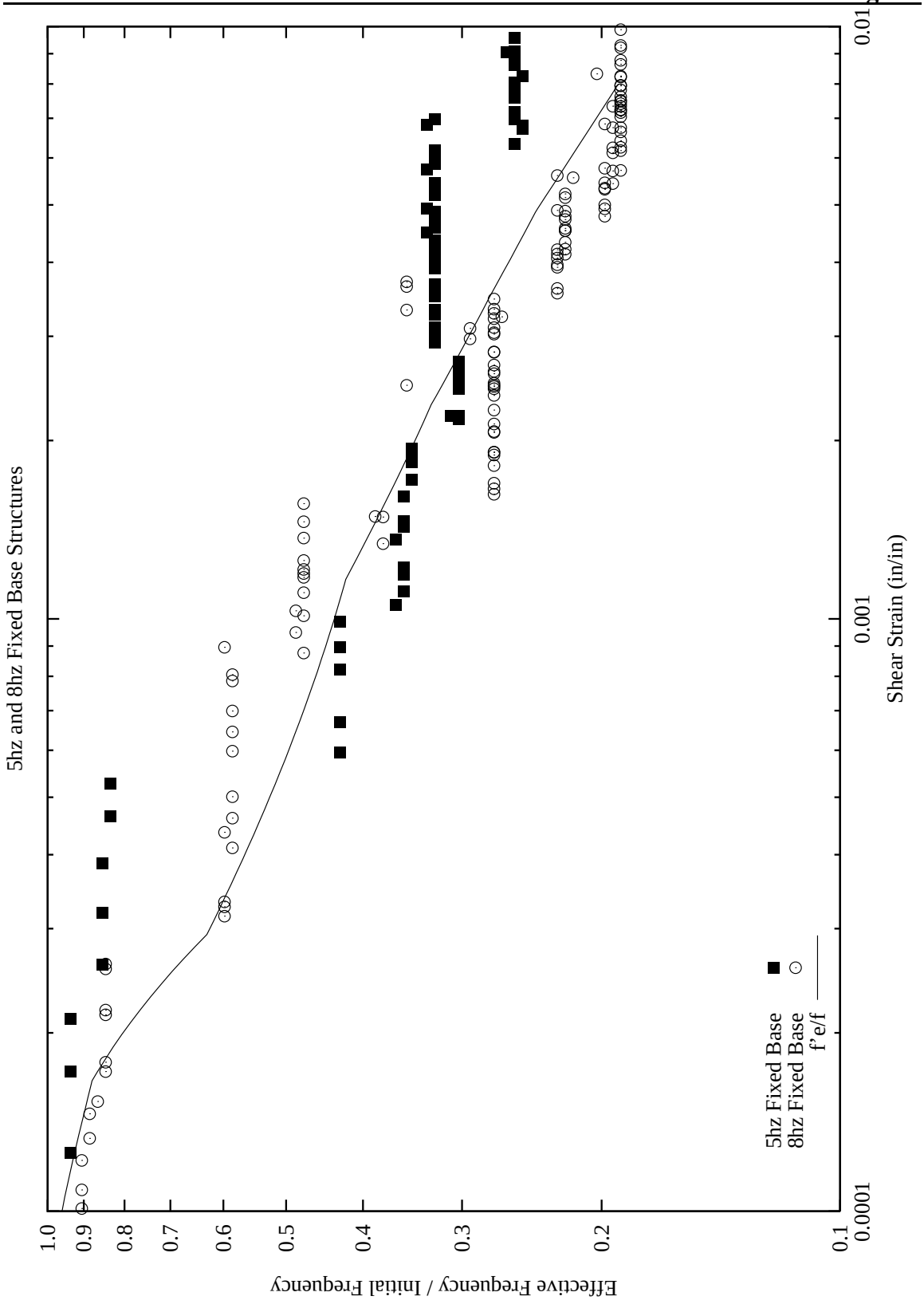

Figure 3.21 Effective Frequency for Fixed Base Structures

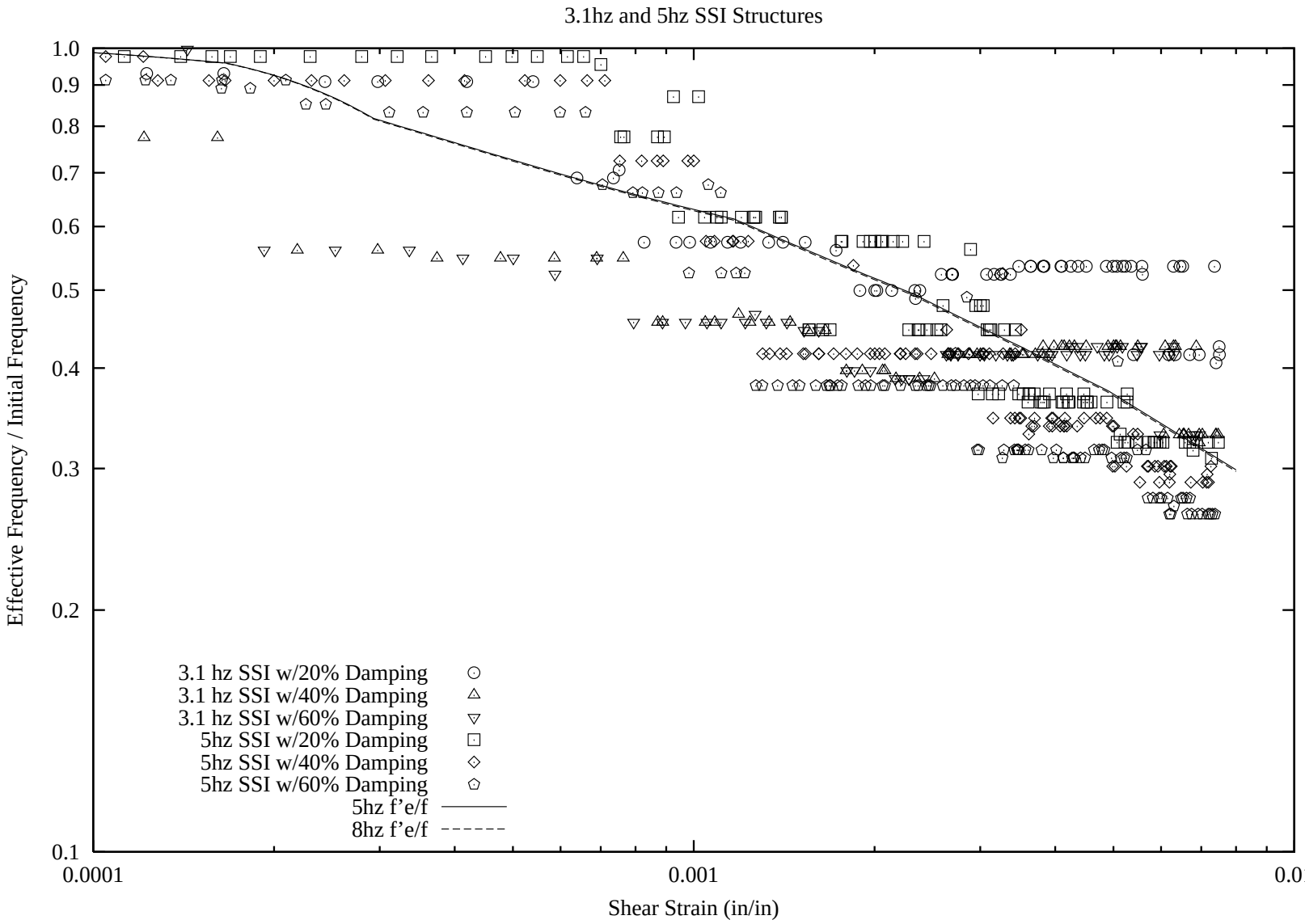

Figure 3.22 Effective Frequency for SSI Structures

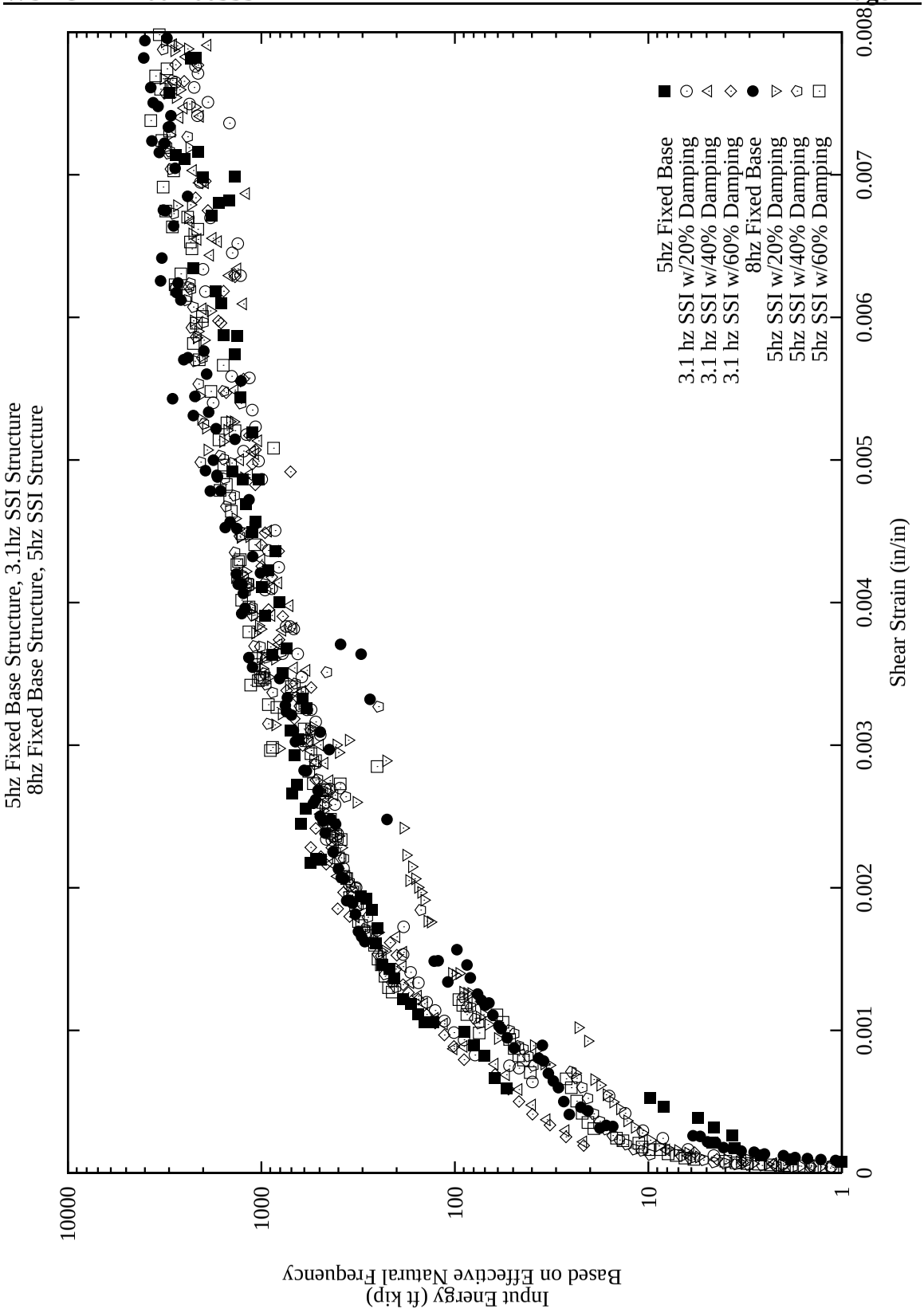

Figure 3.23 Input Energy vs Shear Strain

4.0 Summary and Conclusion

The inelastic force reduction factor, Fμ, is calculated for shear walls with and without the effects of soil flexibility by comparing the calculated elastic to nonlinear responses. Consistent with FEMA-273 and the draft standard [1], wall damage is expressed by a single parameter, shear strain. Fμ is observed to generally increase with increasing amounts of shear strain.

For the structures examined, Soil Structure Interaction did not significantly affect the magnitude of wall shear strain. The scatter in peak shear strain between successive analyses with small differences in input acceleration is on the same order of magnitude as the scatter in peak strain for analyses with and without SSI.

The primary reason that SSI did not have a significant influence on shear strain is because for moderate to large strains the response is dominated by the wall displacement and the soil flexibility is inconsequential. Thus, both the fixed base and SSI structures have similar response.

The effective frequency of each nonlinear structure is determined from in-structure response spectra taken at the top of the wall. As the magnitude of peak shear strain increases the structure'-s effective frequency decreases. For strains near 0.0075 in/in, which corresponds to Limit State A in the draft standard, the effective frequency of fixed base structures is near 25% of the initial frequency. For strains near 0.001 which corresponds to one-quarter of Limit State C in the draft standard, the effective frequency can be 50% of the initial frequency. For moderate to large strains the frequency shift due to SSI is small compared to the frequency shift due to shear wall stiffness degradation.

The nonlinear response spectra are compared to elastic response spectra for a structure which meets the acceptance criteria in the draft standard. The elastic structure response spectra overestimates the response of the nonlinear structure and misses the effective frequency. The difference in both frequency and amplitude are more exaggerated for the fixed base structure than for the SSI structure.

The shear walls examined in this study are clearly in the energy control portion of the input spectra as evidenced by the strong correlation between input energy and wall strain. The equal energy approach yielded reasonable estimates of Fμ whereas the equal displacement approach yielded grossly unconservative Fμ.

SSI did cause a reduction in Fμ. This reduction is not due to a concentration of damage in the shear wall. However, this reduction is due to the reduction in elastic response as soil damping is introduced. The weak / soft story Fμ reduction, given in the draft standard, should not be used to adjust Fμ for SSI.

Overall, the Fμ proposed by the draft standard [1] are conservative for both fixed base and SSI structures. The Fμ are negligibly unconservative for particular combinations of frequency and damping.

5.0 References

1. "Draft – Seismic Design Criteria for Structures, Systems and Components in Nuclear Facilities and Commentary," ASCE, March 2002.

2. DOE-STD-1020-94, "Natural Phenomena Hazards Design and Evaluation Criteria for Department of Energy Facilities," DOE, 1994.

3. N.M. Newmark, W.J. Hall, "Development of Criteria for Seismic Review of Selected Nuclear Power Plants," NUREG/SR-0098, 1978.

4. F. Y. Cheng, G. E. Mertz, M. S. Sheu, J. F. Ger. "Computed versus Observed Inelastic Seismic Low-Rise RC Shear Walls," ASCE Journal of Structural Engineering, Vol 119, No. 11, November 1993.

5. F. Y. Cheng, G. E. Mertz, "Inelastic Seismic Response of Reinforced-Concrete Low-Rise Shear Walls and Building Structures," US Dept. of Commerce, National Technical Information Service, NTIS No. PB90-123217, 1989.

6. F. Y. Cheng, G. E. Mertz "A Computer Program for Inelastic Analysis of 3-Dimensional Reinforced-Concrete and Steel Seismic Buildings," US Dept. of Commerce, National Technical Information Service, NTIS No. PB90-123225, 1989.

7. E. Miranda, V.V. Bertero, "Evaluation of Strength Reduction Factors for Earthquake-Resistant Design," Earthquake Spectra, Vol 10, No. 2, May 1994.

8. G. E. Mertz, T. W. Houston, "Force Reduction Factors for the Structural Design and Evaluation of Facilities Containing Nuclear and Hazardous Materials," WSRC-TR-2001-00037, March, 2001.

9. R.P. Kennedy, S.A. Short, K.L. Merz, F.J. Tokarz, I.M. Idriss, M.S. Power, K. Sadigh, "Engineering Characterization of Ground Motion Task I: Effects of Characteristics of Free-Field Motion on Structural Response," NUREG/CR-3805, May, 1984.